International Journal of Greenhouse Gas Control 19 (2013) 756–774

Contents lists available at ScienceDirect

International Journal of Greenhouse Gas Control

journal homepage: www.elsevier.com/locate/ijggc

Geological modelling of the Triassic Stuttgart Formation at the Ketzin CO_2 storage site, Germany

Ben Norden [a,*], Peter Frykman [b]

[a] GFZ Helmholtz Centre Potsdam, German Research Centre for Geosciences, Section 4.1 Reservoir Technologies, Telegrafenberg, 14473 Potsdam, Germany
[b] GEUS Geological Survey of Denmark and Greenland, Ø. Voldgade 10, 1350 Copenhagen, Denmark

ARTICLE INFO

Article history:
Received 4 July 2012
Received in revised form 18 March 2013
Accepted 3 April 2013
Available online 29 May 2013

Keywords:
Stochastic modelling
Facies modelling
Fluvial environment
Channel deposit
CO_2 storage

ABSTRACT

At Ketzin, about 25 km west of Berlin (Germany), the saline aquifer of the Triassic Stuttgart Formation is used for a carbon dioxide storage research project. The formation is lithologically very heterogeneous, reflecting a complex fluviatile facies distribution pattern. We focused on the development of a primary geological reservoir model as commonly employed for dynamic modelling during the planning and early injection stages of a storage project. Due to the need to capture the complex geometrical structure of the Stuttgart Formation, despite limited availability of exploration data, stochastic modelling techniques were employed. Firstly, we modelled the facies architecture of the reservoir and, secondly, assigned porosity and permeability values to the facies types included in the model. Petrophysical parameters for each facies type were quantified using site-specific porosity histograms and related permeability functions. The comparison of dynamic flow simulation results and well-test interpretations, and furthermore with the first observed monitoring data, helped to focus the modelling work and to adjust monitoring plans. Modelling is understood as an iterative process, both with respect to data arrival and progressively improving the understanding of the reservoir, but also with respect to the problem which the model is being designed to address.

1. Introduction

A sound geological model including the geometry of all relevant geological bodies and their petrophysical properties is a prerequisite for simulating and forecasting dynamic processes arising from the utilization of the subsurface (Johnson, 2009; Eigestad et al., 2009). Subject to the purpose of the applied simulation, different models need to be considered. For complex geological settings in particular, different scales and resolutions must be considered when describing different scales. Investigations of the small-scale and/or short-time behaviour (e.g. around boreholes during injection or production of fluids) require a different model design compared to investigations of the large-scale and/or long-time behaviour (e.g. movements across faults and hydraulic compartments during production or even geological time scales). Although site-specific subsurface knowledge and data is limited, geological models are nevertheless expected to live up to demanding requirements. The challenge is, therefore, to integrate and utilize the full range of available local and regional geological information to produce a model describing subsurface architecture and properties in a consistent manner (Wu et al., 2005; Kaufmann and Martin, 2008).

In this paper we present the development of a reservoir model of a saline aquifer used for the injection of carbon dioxide (CO_2) close to the village of Ketzin, Germany. The geological modelling of the site exhibits some features and challenges typical for reservoirs in an early stage of utilization for CO_2 storage, hydrocarbon production or extraction of geothermal heat. Based on former reconnaissance exploration data, a target reservoir is expected in a certain depth interval. In addition, a heterogeneous lithological sequence is documented by borehole data and could be interpreted in a general geological (sedimentological) context. The data is, however, very scattered and/or scarce, resulting in a very poor knowledge of the exact geological setting on the local scale. Under these conditions, stochastic simulation techniques are helpful tools to draw possible pictures of the subsurface. In order to apply such modelling approaches, a clear conceptual understanding of the geological setting becomes important. The resulting geological models do not claim to represent the in situ situation exactly as it is present in the underground, but presents a conceptual picture, taking into account the complexity of the reservoir as it could be deduced from the data available. Furthermore, it should be consistent with

* Corresponding author. Tel.: +49 331 288 1578; fax: +49 331 288 1450.
E-mail addresses: ben.norden@gfz-potsdam.de (B. Norden), pfr@geus.dk (P. Frykman).

1750-5836 © 2013 The Authors. Published by Elsevier B.V. Open access under CC BY license.
http://dx.doi.org/10.1016/j.ijggc.2013.04.019

recorded production or monitoring data from the reservoir. In this paper, the performed geological modelling procedure for the set-up of the first reservoir model of the Ketzin site, including local well and site data prior to CO_2 monitoring data, is described in detail aiming to demonstrate the possibilities and uncertainties of reservoir models dealing with geometrical and lithological complex reservoirs. The study also shows the large diversity of data, from the regional framework to selected analogues for deposition and properties, which has to be included, especially when dealing with saline aquifers that usually have sparse information. Modelling is performed using the Petrel™ software suite (courtesy of Schlumberger-SIS). The work forms the foundation for later re-evaluations of the local geological model as soon as more detailed monitoring data will become available.

2. CO_2 injection in Ketzin

At Ketzin, the first European on-shore CO_2 injection research storage site was established (Förster et al., 2006). The site is located on an anticlinal structure of the Northeast German Basin (NEGB), about 25 km west of Berlin (Fig. 1). The project was initiated in 2004 and injection of CO_2 started in 2008. Whereas the Jurassic aquifers at depths of 250–400 m were used as a coal gas and natural gas storage from the 1970s until 2000, the target reservoir for the CO_2 injection is located in the deeper and less explored Triassic Stuttgart Formation at a depth of 625–700 m. As part of the European project CO_2SINK, three wells (one injection and two observation wells) were drilled into the Stuttgart Formation in 2007 (Schilling et al., 2009). At the same time the wells acted as exploration wells and enabled a more detailed characterization of the Stuttgart Formation at the Ketzin site based on log and core data (Prevedel et al., 2009; Förster et al., 2010; Norden et al., 2010). As expected from other boreholes of the NEGB, the Stuttgart Formation is lithological very heterogeneous. Several metres of sandy channel-facies rocks with good reservoir properties alternate with muddy floodplain-facies of poor reservoir quality. Despite the complex reservoir setting, the Ketzin site was chosen as a CO_2 injection research storage site for mainly four reasons. Firstly, the anticlinal structure enables a controlled propagation of injected CO_2 towards the top of the anticline. Secondly, due to the operation of the former natural gas storage, local infrastructure and facilities can be used for the project. Thirdly, one of the project partners is holding the mining rights of the site, enabling the timely realization of the project. Finally, the close proximity to a large metropolitan area enables the evaluation of the public acceptance of a CO_2 storage site.

Within the research activities at the site, particular attention is paid to the monitoring component of geological CO_2 storage. In the three CO_2SINK wells, fibre-optic sensor cable loops for distributed temperature sensing (DTS), vertical electrical resistivity arrays for electrical resistivity measurements, and fibre-optic pressure/temperature sensors (at injection well only) were installed permanently (Prevedel et al., 2009). Additionally, seismic monitoring techniques are forming an important component of the monitoring programme. Applied methods include cross-well, vertical seismic profile (VSP), moving source profiling and 2D and 3D time-lapse techniques. In 2004, a pilot seismic study was carried out to determine acquisition parameters (Yordkayhun et al., 2009a). This survey was followed by a 3D baseline seismic survey with 12 km^2 of sub-surface coverage in 2005 (Juhlin et al., 2007). The 3D survey revealed clear E–W trending faults on the crest of the Ketzin anticline and a clear signature from remnant gas in the sandy Jurassic formations originating from the past natural gas storage operations. One interpretation of seismic attributes yielded some first indications that the sandy reservoir channels within the heterogeneous Stuttgart Formation may affect the seismic amplitude of reflections from within this unit (Juhlin et al., 2007; Kazemeini et al., 2009).

Injection started in June 2008 (Schilling et al., 2009). After injection of more than 62,000 tonnes (until May 2012) into the Stuttgart Formation, the injection was run at a stable scheme and with no irregularities. From May 2012 to January 2013 injection was orderly shutdown for other technical reasons. Soon after the injection started in the injection well CO2 Ktzi 201/2007 (short name: Ktzi-201), the breakthrough of CO2 at the first observation well (CO2 Ktzi 200/2007; short name: Ktzi-200) 50 m away from the Ktzi-201 well was observed in mid of July 2008 (after 21.7 days and 531.5 metric tonnes of injected CO_2). The arrival of CO_2 in the second observation well (CO2 Ktzi 202/2007; short name: Ktzi-202) 110 m away from the injection well was observed much later, in April 2009 (after 271 days and 11,000 tonnes of injected CO_2). Further details on the first years of operation are presented by Schilling et al. (2009), Würdemann et al. (2010), and Martens et al. (2012). Various numerical simulations have been performed for the Stuttgart Formation (Kopp et al., 2009; Lengler et al., 2010; Kempka et al., 2010; Pamukcu et al., 2011) in order to reach a better understanding of the reservoir behaviour and for ensuring a continuous and safe CO_2 injection. These studies focused on different aspects of modelling and investigated the CO_2 injection in the complex aquifer structure on different scales, by also testing different geological presumptions and models. The work of Kopp et al. (2009) presents first results for a general CO_2 storage capacity estimation of the Ketzin site based on a geological model like the one documented here, whereas Lengler et al. (2010) studied the general impact of spatial variability in the petrophysical properties by applying stochastic methods to the Ketzin reservoir formation using a Monte Carlo approach. Kempka et al. (2010) used a geological model based on the same general geological assumptions like Kopp et al. (2009) for testing different numerical simulation codes and their ability to give reliable estimates of CO_2 propagation with time. Finally, Pamukcu et al. (2011) used another realization of this model to perform dynamic simulations and history matching for Ketzin. However, the principal geological modelling procedure is not described in any detail in these references. In order to close this gap for the Ketzin site, in this paper we are presenting the geological modelling process which was followed to set-up the first site-specific geological model, i.e. prior to the integration of operational and monitoring site data.

3. Geology

The Ketzin site is located in the North-East German Basin (NEGB, Fig. 1), a sub-basin of the Central European Basin System the formation of which was initiated during the latest Carboniferous to earliest Permian time. The sedimentary succession of the basin comprises up to 6500 m of Permian to Quaternary age sediments (Hoth et al., 1993). At Ketzin, the sedimentary succession exhibits a thickness of about 4000 m. In the Roskow-Ketzin area, diapirism of Permian (Zechstein) salt has caused deformation of Triassic and Lower Jurassic formations generating a gently dipping, ENE–WSW-striking double anticline. Transgressive sediments of the Oligocene (Rupelton) resting above Lower Jurassic sediments form the first formation unaffected by anticlinal uplift (Förster et al., 2006). The Tertiary deposits are in turn overlain by unconsolidated Quaternary sediments. The reservoir for CO_2 storage is located within the Middle Keuper (Upper Triassic) section, in the Stuttgart Formation with injection at depths of 625–700 m. The Stuttgart Formation is overlain by the Weser Formation, which acts as the immediate caprock of the reservoir. The extent of the Roskow-Ketzin double anticline is illustrated by the structure map of a pronounced

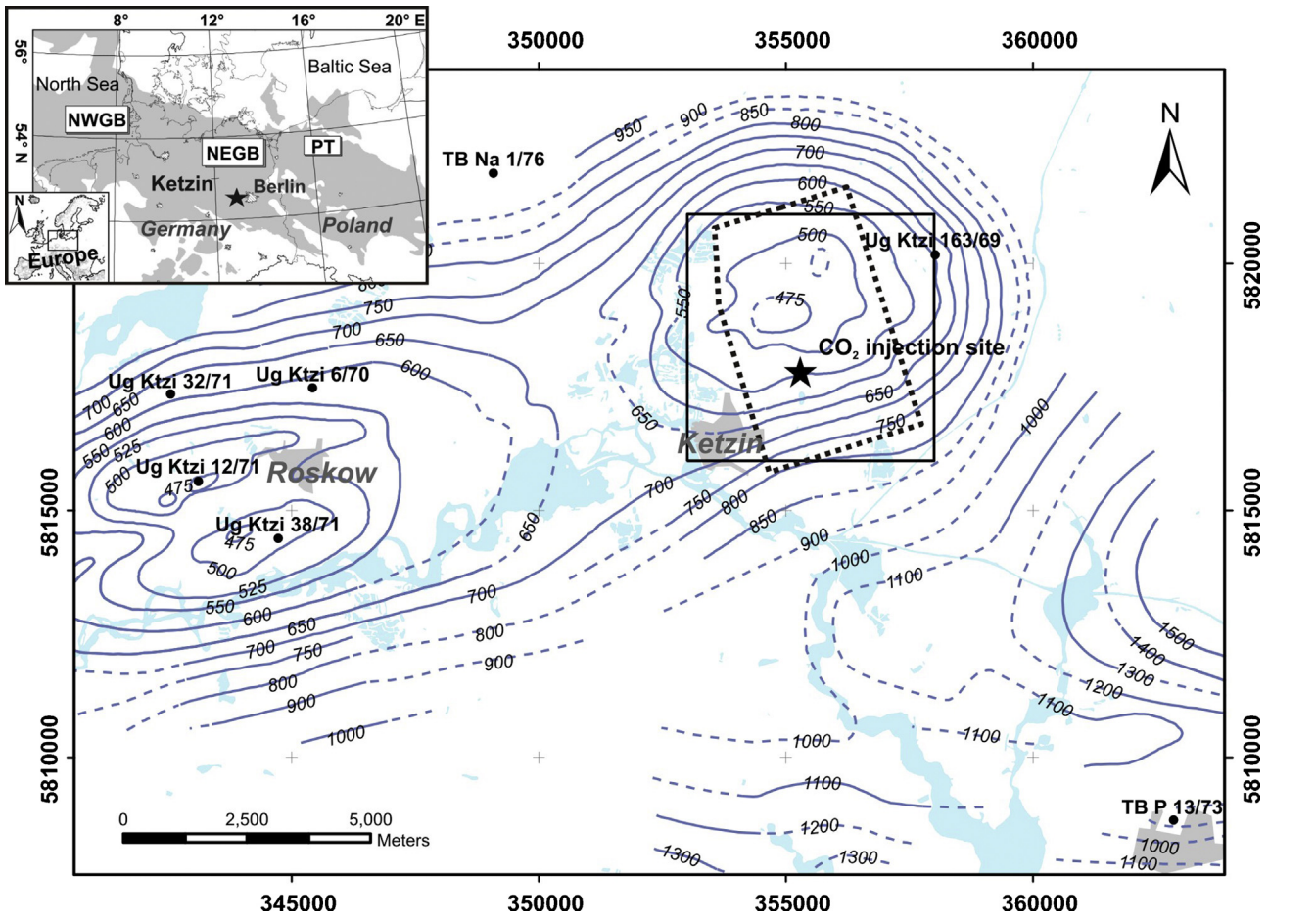

Fig. 1. Structure of the Roskow-Ketzin double anticline, highlighted by the isolines (metres below ground level) of the strongest seismic reflector of the Triassic ("K2 horizon", uppermost Weser Formation). Shown are the locations of former exploration boreholes penetrating the Stuttgart Formation (dots) and the location of the Ketzin CO_2 boreholes (star), the extension of the 3D seismic data (stippled black lines), and the reservoir model domain size (black square). For geographic orientation, main waters and the location of the villages Roskow and Ketzin are given. Coordinate System: UTM WGS 1984, Zone 33. The inlet map shows the extent of the European Permian Rotliegend Basin (grey-shaded) and the location of the Ketzin site in the Northeast German Basin (NEGB), which is situated between the Northwest German Basin (NWGB) and the Polish Trough (PT).

seismic reflector, the K2 horizon which picks up a 10–20 m thick anhydrite/gypsum at the top of the Weser Formation, about 80 m above the Stuttgart Formation (Fig. 1). Further up in the sequence, the Jurassic age Sinemurian/Hettangian reservoir sands, situated at depths of 250–400 m, were used as a storage facility for coal gas and natural gas for about 30 years.

Based on the 3D seismic campaign (Juhlin et al., 2007), a structural model of the Ketzin site was developed. The seismic survey, acquired in the fall of 2005, covers an area of approximately 15 km^2 in the central and southern part of the Ketzin structure (Fig. 1). The initial interpretation of the seismic data includes the mapping of three main reflection horizons according to Reinhardt (1993): the T1 reflector (base of soft rock sediments), the K2 reflector (Top Weser Formation), and the K3 horizon (near base of Stuttgart Formation) as well as the mapping of four further less pronounced horizons including the expected Top Stuttgart horizon, which was picked based on the drilling results of the Ketzin boreholes. The seismic data confirms the presence of a fault zone at the top of the anticline structure, about 1.5 km north of the CO_2 injection site. The outline of the WSW–ENE trending fault zone (the Central Graben Fault Zone, CGFZ; Juhlin et al., 2007; Fig. 2) is controlled by a series of discrete normal faults. The faults are well developed in the Triassic and Jurassic section but seem to die out quickly in the Tertiary Rupelian clay (Yordkayhun et al., 2009b,c). The main bounding faults have throws in the order of up to 30 m in the Jurassic section (Juhlin et al., 2007). Beside the CGFZ, a number of faint, SE- to SSE-striking lineaments on the Top Weser may indicate the presence of small-scale faults with a throw of 1.5–3.0 m (Juhlin et al., 2007). These faults seem not to be present, however, in the vicinity of the injection site.

3.1. Stratigraphy, facies, and lithology of the Stuttgart Formation

The Middle Keuper in Northern Germany is subdivided into the Grabfeld Formation, the Stuttgart Formation, the Weser Formation, and the Arnstadt Formation. Continental playa-type sedimentation prevails in all units, except for the Stuttgart Formation which shows a change in depositional style from playa to fluvial environment (Beutler et al., 1999). The *Stuttgart Formation* consists of flood plain siltstones and mudstones with embedded channel sandstones. In distinct areas, the channel sandstones are more frequent, reflecting channel-belt fairways ("Strangfazies" of Beutler, 2002). These often exhibit S to SW-oriented paleocurrent directions reflecting sediment transport from northern and eastern Europe across the German Keuper basin (Beutler and Häusser, 1982). However, flow directions for the northern part of Germany cannot be determined due to a lack of outcrops. The lateral extent of the channel belts, formed by amalgamation of individual fluvial channels, is highly variable. Basin-wide the Stuttgart Formation is on average only 20–100 m thick (Beutler and Tessin, 2005). The low thickness as

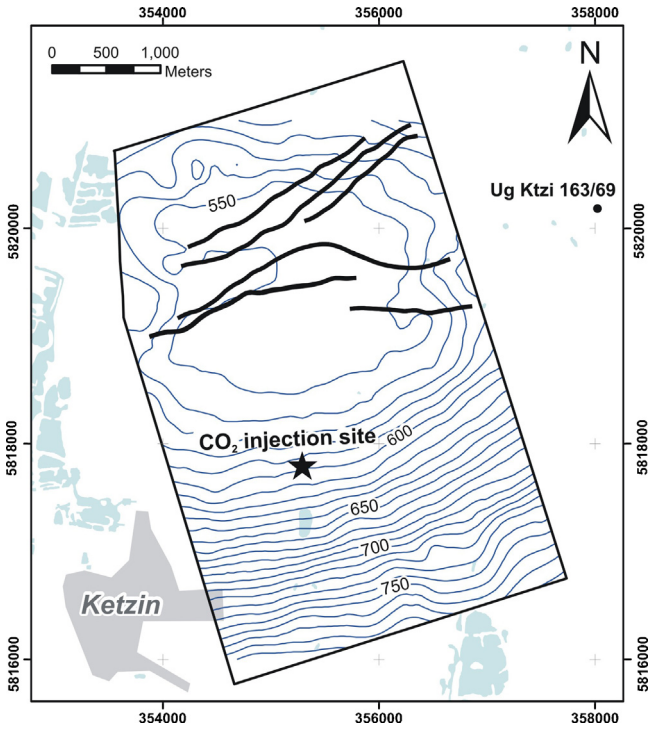

Fig. 2. Interpreted depth of the top Stuttgart Formation (in metres below ground level) and mapped faults of the Central Graben Fault Zone (CGFZ; Juhlin et al., 2007). The bold star marks the location of the boreholes used for injection and monitoring of CO_2. Coordinate System: UTM WGS 1984, Zone 33.

well as the basin-wide homogeneous grain size of its immature sandstones, indicates rapid transport and deposition, i.e. for a substantial drop of base level (Aigner and Bachmann, 1992). Thus, the Stuttgart Formation represents a Lowstand System Tract (Aigner and Bachmann, 1992). Another factor that could contribute to the immature composition is the interpretation of the deposition of the Stuttgart sands during a slightly more humid climatic period. This interpretation is corroborated by the presence of spores from plants only growing in very humid conditions (Hornung and Aigner, 2002). More humid conditions would generally increase erosion, run-off and transport potential of the fluvial systems (Hornung and Aigner, 2002). Studied quarries and boreholes in Thuringia, approximately 300 km south of Ketzin, show a variable distribution of sandy channel and muddy interfluves deposits. No distinct levee and crevasse successions in the classical sense have been described in Central Germany (Shukla et al., 2010): the channel bodies are always flanked by thick units of silt and ripple cross-laminated fine sand. In southern Germany, however, levee-crevasse deposits were described by Ricken et al. (1998). According to Shukla et al. (2010), depending on residence time, the channel belts evolved and aggraded systematically producing multi-storied sand bodies. These display progressively thinner stories mainly in response to decreased sediment flux and increased sediment/water ratio in the channels caused by changing climate affecting the base level.

3.2. The Stuttgart Formation in Ketzin

The Ketzin site is considered to be located within a channel belt fairway (Förster et al., 2010). Fig. 3 shows the expected sand distribution close to Ketzin (Beutler, 2002) and the borehole data of the larger Ketzin area. Beutler (2002) mapped the sand occurrence based on the estimated sandstone content which he calculated using available log data (i.e. the natural gamma-ray log). The borehole locations with an interpreted sand content above 60% were used to guide the interpretation of channel positions assuming that the general flow direction follows a N–S trend.

At Ketzin, the Stuttgart Formation is 71–74 m thick (Förster et al., 2010), which is in the similar range to what was encountered in neighbouring boreholes (75–85 m, Fig. 4). The drilled lithological profiles are, however, very different in detailed stacking patterns, reflecting the lateral changes in a fluvial depositional environment. In contrast to most of the other boreholes (except for the TB Na 1/76 borehole), the Ktzi-200, Ktzi-201 and Ktzi-202 boreholes show the highest sand content in the uppermost part of the Stuttgart Formation. In the three boreholes at the CO_2 injection site in Ketzin, the net-to-gross ratio (N/G-ratio) amounts to 0.26–0.35 (Fig. 4). Thus, the Ketzin site does not fit into the channel belt definition of Beutler. The N/G-ratio of sandstone to muddy floodplain deposits from the other boreholes varies from 0.07 (TB P 13/73) to 0.64 (Ug Ktzi 163/69; Fig. 4). The mean N/G-ratio of all boreholes amounts to 0.33. Although the data from the Ug Ktzi 163/69 borehole 4 km NE of Ketzin shows a high N/G-ratio, it does not plot into the channel facies fairway of Beutler (Fig. 3). This suggests that the overall reliability of such general compilations may not be consistent when focusing on the local scale.

3.2.1. Lithology of the Stuttgart Formation

The drilled Stuttgart Formation in Ketzin is dominated by muddy sediments of the flood plain facies. Subordinate channel sandstones are also developed (Fig. 4). For the flood plain overbank facies, mottling and convolute or ruptured lamina structures could be observed (Fig. 5), with also pyrite being present. While anhydritic lenses are common in the mudstones of the Weser Formation and the upper part of the muddy Stuttgart Formation, anhydrite is less frequent in the deeper part of the Stuttgart Formation. For these deeper parts, anhydrite is mainly present as pore-filling rock cement in certain sandstone intervals (Fig. 5). Thin coaly horizons (1–5 cm) are typically interbedded with fine-grained overbank sediments. Vitrinite reflectance data show values of 0.6–0.9%Ro, indicating maximum burial temperatures of 85–135 °C according to Harvey and Dillon (1985). Liptinite macerals (tenuispores) are also present, documenting the formation of the coal streaks by allochthonous processes like the accumulation of windblown spores (Miall, 1996). Pedogenic marks (plant roots) and iron nodules indicate the occasional exposure of the floodplain deposits.

The standard logging data does not allow distinguishing different parts of the channel infill in great detail. However, despite the high content of accessory minerals (clay) present in the sandstone, the GR log shows different baselines in accordance with the interpreted overbank and channel environments (Fig. 5). The deep resistivity (Rdeep), the neutron porosity (Phi-NN), and the bulk density (DEN) readings provide further indications especially for the anhydrite cemented intervals. The Rdeep and DEN reading show a weak bottom up increasing trend for the channel fills (red arrows in Fig. 5) and do indicate some kind of cyclicity for the overbank sediments (e.g. at 654–658 m). From core analysis, both fining and coarsening upward sequences may be observed in parts of the channel fills. The sandstones of the Stuttgart Formation are dominantly fine-grained and well to moderately well sorted. They classify as feldspathic litharenites and lithic arkoses (Förster et al., 2010) and contain a rich diversity of accessory minerals. Sandstone colour varies from grey, olive, and ochre to dark brown and dark reddish brown, showing sometimes mottling. The sandstone is massive (structureless) or shows low-angle and high-angle planar lamination, cross bedding, and often horizontal laminations (Fig. 5). In certain intervals, mudclasts could be observed. Palaeocurrent directions determined on cross bedding show a NW–SE direction (Fig. 5). The general azimuth direction determined from structural

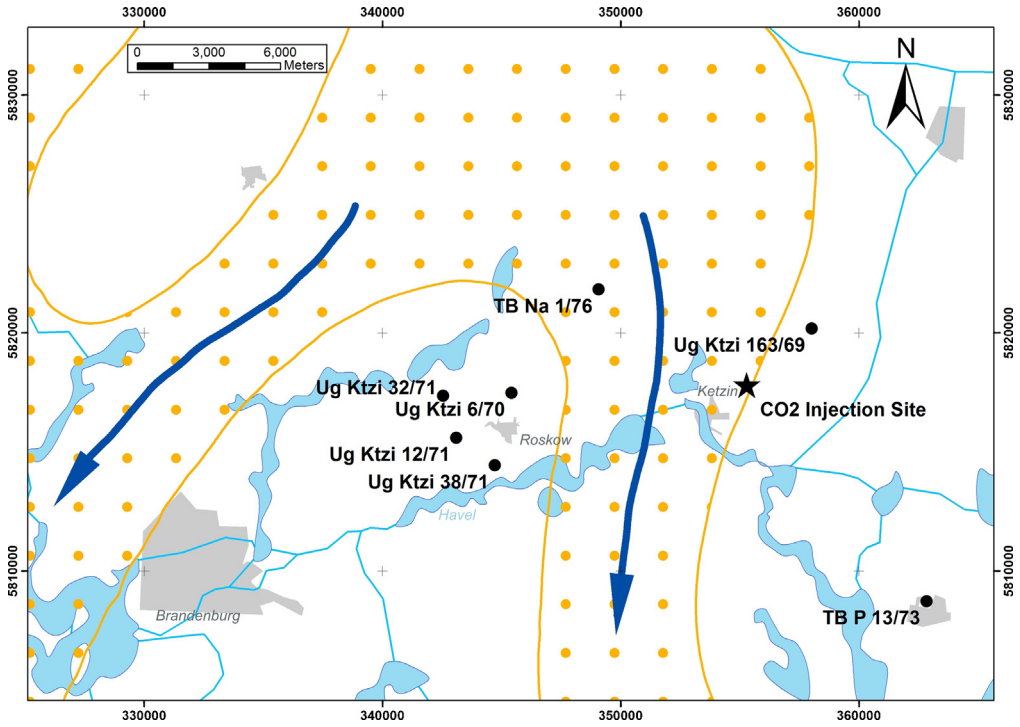

Fig. 3. Facies map of the Stuttgart Formation according to Beutler (2002) showing the distribution (dotted area) and flow direction (long arrows) of the channel belts together with the locations of existing boreholes (black dots). Underlain are topographic features (recent water bodies and city boundaries). Coordinate System: UTM WGS 1984, Zone 33.

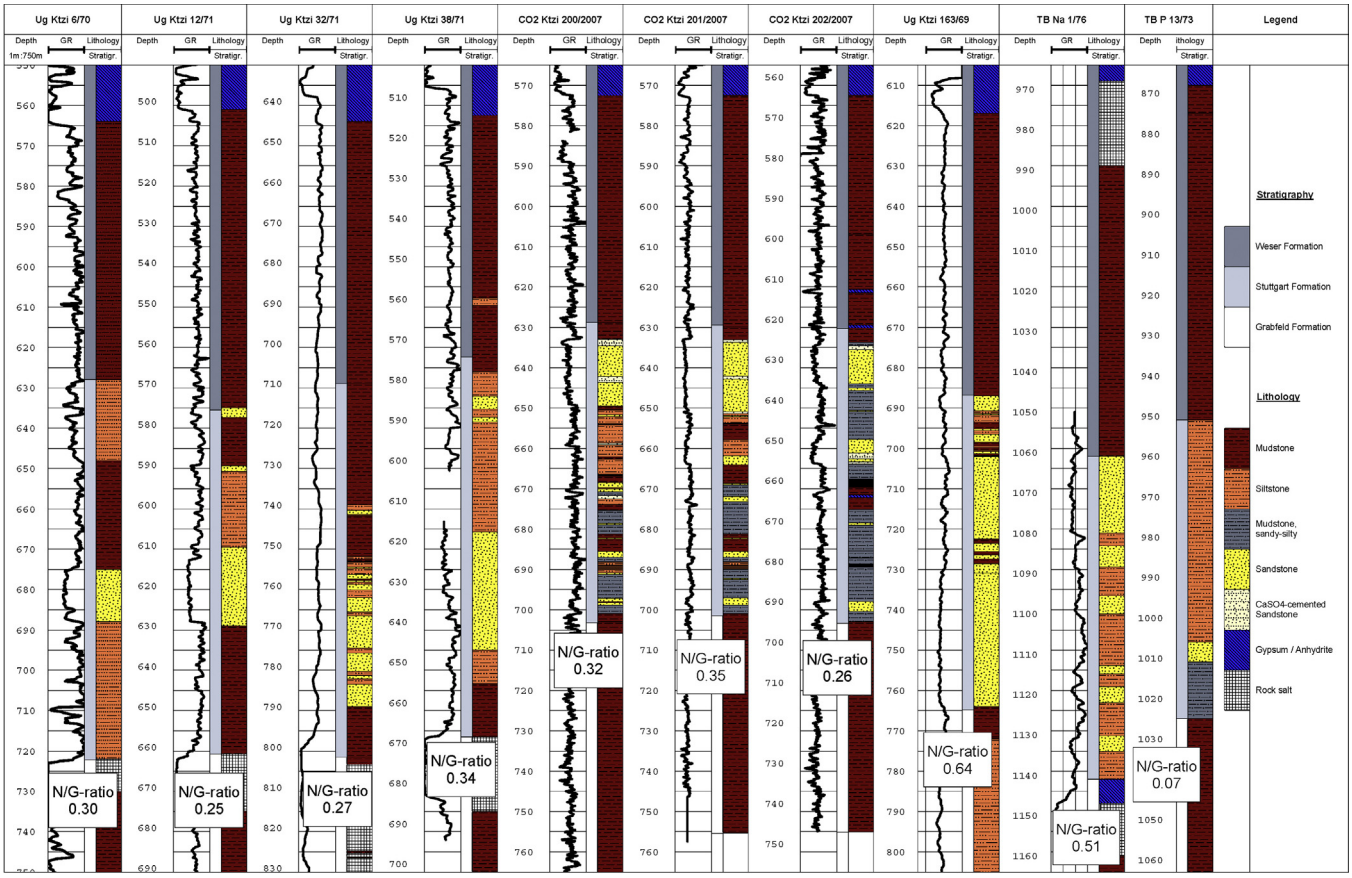

Fig. 4. Lithological profiles of the Stuttgart Formation from boreholes shown in Fig. 3.

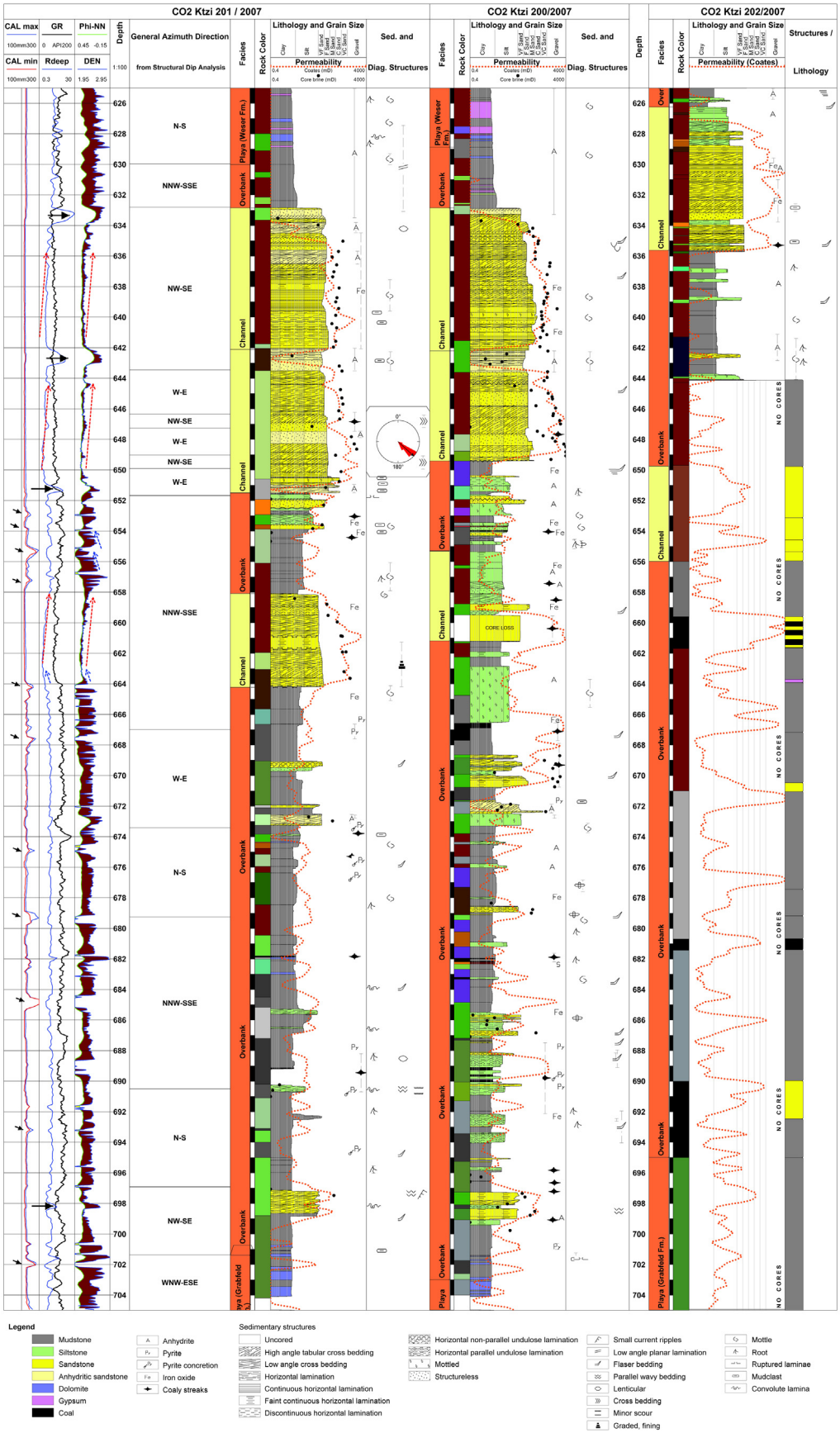

Fig. 5. Composite plot of well-log data, lithological and sedimentological descriptive data, and derived facies data of the CO2 Ktzi 201/2007, CO2 Ktzi 200/2007, and CO2 Ktzi 202/2007 boreholes. (For interpretation of the references to colour in text, the reader is referred to the web version of this article.)

Table 1
Mean set thickness (s_m), standard deviation of s_m (s_d), mean dune height (h_m), and mean bankfull depth (d) determined for the channel sandstones of the CO_2 Ketzin boreholes.

Borehole (channel)	Depth range (m)	s_m (m)	s_d	h_m (m)	d (m)
Ktzi-200					
Channel A	633–642	0.21	0.76	0.62	3.7
Channel B	642–649	0.28	1.04	0.85	5.2
Ktzi-201					
Channel A	633–642	0.35	0.51	1.02	6.1
Channel B	642–621	0.37	0.79	1.08	6.5
Ktzi-202					
Channel	626–636	0.32	0.84	0.93	5.6

dip analysis of the electrical image plot of the Ktzi-201 borehole shows mainly an orientation between N–S and W–E.

3.2.2. Interpretation of the depositional system

The high degree of variability in channel morphology along channel lengths and with time observed in studies of modern fluvial channels, can, for the most part, not be recognized in ancient fluvial deposits (Ethridge, 2011). It is therefore difficult to deduce the characteristic setting for the Ketzin site based on the limited subsurface data available. There are, however, some indicators that could be used for describing the depositional setting. Firstly, the sandstone sections of the upper part of the Stuttgart Formation drilled in Ketzin show vertically stacked bed sets with different bedforms and changing dip directions. Maximum channel sand thickness amounts to about 4–10 m in Ketzin (Ktzi-201), whereas in the Ug Ktzi 163/69 borehole nearly 4 km apart from the Ketzin pilot site and unfortunately lacking of any detailed core data, the total sand thickness exceeds more than 35 m. According to Gibling (2006) and Shukla et al. (2010) these observations may suggest that deposition of sand bodies occurred in braided to meandering rivers. From the borehole records we could neither prove the existence of levee and crevasse sequences nor exclude their existence. These types of deposits were not found by Shukla et al. (2010) in outcrops in Central Germany, but are documented from outcrops in south Germany (Ricken et al., 1998). We therefore assume that such sequences are less important at Ketzin. Secondly, the generally fine-grained sand supports an interpretation of a low gradient, low fluid-flow velocity of paleochannel system. Therefore, the system at Ketzin is likely to be a dominantly meandering depositional system or low-flow secondary channels of a braided system. At Ketzin, the silty sandstones and siltstones encountered in the lower part of the Stuttgart Formation are interpreted as overbank sediments due to their minor thickness and their mineralogy (Förster et al., 2010). They may also partly reflect depositions of floodplain channels (Gibling, 2006). The upper relatively thick sandstone section is interpreted as a migrating channel belt. Thirdly, from the analysis of cross-bed thickness and flow depth, one can estimate paleochannel depth (Bridge and Tye, 2000; Leclair and Bridge, 2001). Based on the paleochannel depth, channel-belt width can be estimated by using empirical equations (Bridge and Mackey, 1993). Although these equations have considerable errors, they may provide a first estimate of channel architecture at Ketzin. By applying this approach on the three Ketzin boreholes, the mean set thickness of the channel sandstones units and the respective mean dune height was determined (Fig. 5 and Table 1). The set thicknesses were determined using the core descriptions available for all CO_2 Ktzi boreholes. In addition, computer-tomography (CT) images from the sandstone section of the Ktzi-200 borehole and the high-resolution image log of the Ktzi-201 borehole helped in delineating the sedimentary sequence and the internal layering, which was often not easy to observe directly on the full core (Fig. 6). Mean set thickness varies between 0.21 m and 0.37 m, yielding a mean dune height

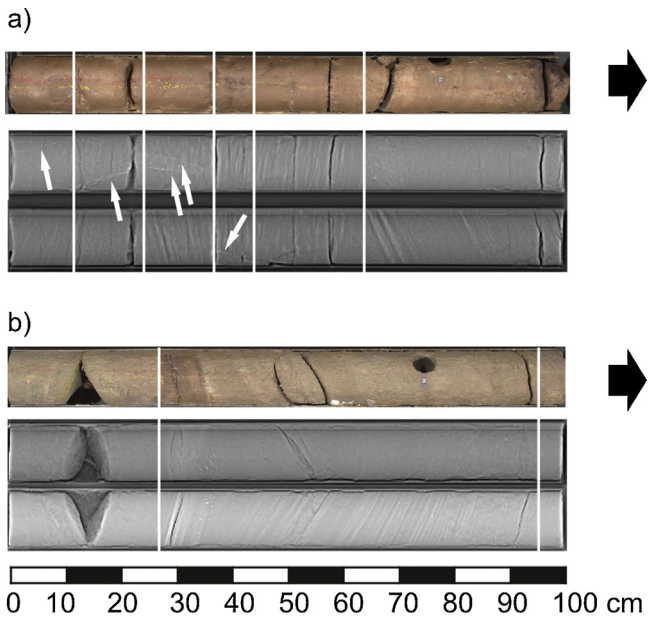

Fig. 6. Examples of computer-tomography (CT) images of cores from the CO_2 Ktzi 200/2007 borehole illustrating the internal layering of the sandstones. Shown are a top view image of the core and two CT scans of different angles, set thicknesses (white line) and orientation (black arrows show down): (a) Ktzi 200-13_1 (635.65–636.65 m), white arrows mark steep dipping anhydritic cemented fractures; (b) Ktzi 200-16_2 (645.60–646.60 m), below a massive sandstone, a bedding sequence with increasing dipping could be observed.

of 0.62–1.08 m according formula (6) of Leclair and Bridge (2001). This range corresponds to a mean bankfull depth of 3.7 m–6.5 m using Eq. (3a) of Bridge and Tye (2000). Based on the formula given by Bridge and Mackey (1993), the range of channel-belt width (W) is predicted to be 631–2495 m. Thus, the ratio of W to channel thickness (T) show a considerable range of 63 (631/10) to 624 (2495/4), quite reasonable for meandering rivers (see e.g. Gibling, 2006).

Beside borehole data, the 3D seismic data of the Ketzin site was utilized to identify facies distribution patterns in the Stuttgart Formation. Although the sand bodies cannot easily be mapped by conventional seismic methods, Juhlin et al. (2007) presented a summed amplitude map indicating the possible distribution of reservoir bodies for the entire formation, whereas Kazemeini et al. (2009) applied the continuous wavelet transform on the seismic data for the expected uppermost part of the Stuttgart Formation. On the decomposed common frequency maps using Mexican Hat wavelets (Fig. 7) a possible curved channel feature is visible indicated by a NE–SW trend of brighter amplitudes in the northern part of the seismic survey, which turns into a NW–SE trend for the southern part of the investigated area, where the CO_2 injection site is located. The width of this presumed channel is in the order of 800–1000 m. Although there is some uncertainty with respect to the interpretation of the seismic results, the orientation and width of the assumed channel are in agreement with the estimates based on the borehole data.

4. Geological modelling

The Ketzin seismic 3D data is not able to resolve the internal structure of the Stuttgart Formation in any detail, and the borehole data from the Stuttgart Formation is not supplying sufficient information allowing a deterministic modelling of the Stuttgart Formation. Therefore, a geostatistical approach is needed to describe the facies distribution and the reservoir architecture of the formation. In the particular case of CO_2 injection into a saline aquifer, it may be possible to qualify the geostatistical model

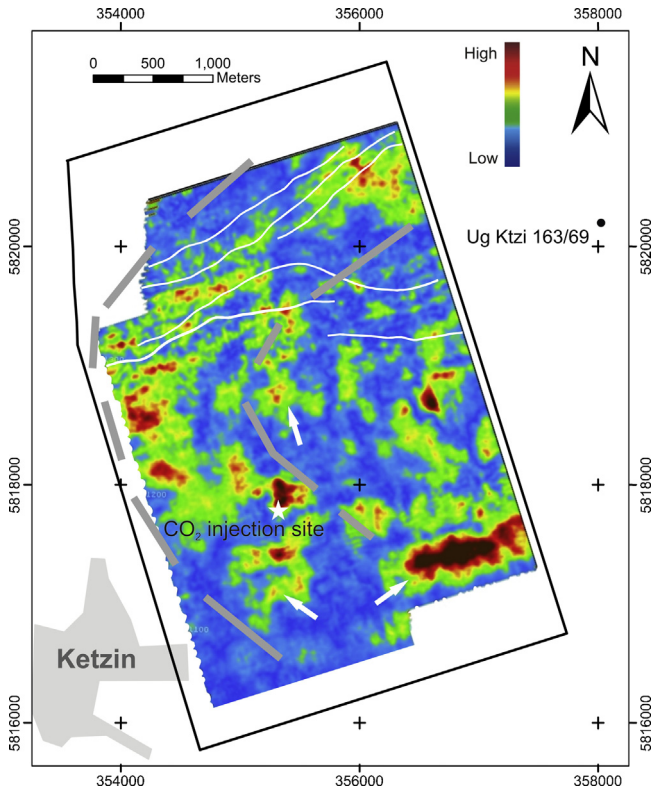

Fig. 7. Decomposed common frequency horizon maps using Mexican Hat wavelets on a horizon 45 ms above Base Stuttgart (ca. 12 m below Top Stuttgart, similar image given by Kazemeini et al., 2009). Fault traces are shown by white lines. White arrows mark features which are interpreted as noise in the data (Kling, personal communication, 2011). Greyish lines indicate the interpreted channel belt geometry (Kling, personal communication, 2011 and Kazemeini et al., 2009). Coordinate System: UTM WGS 1984, Zone 33. (For interpretation of the references to colour in this figure legend, the reader is referred to the web version of this article.)

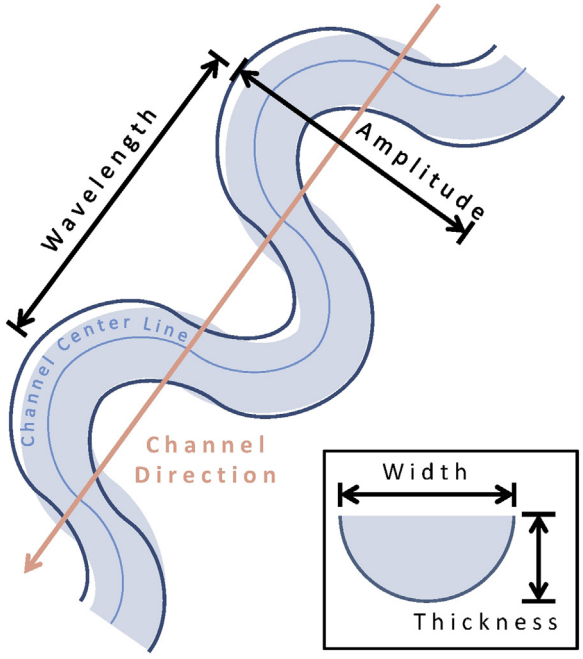

Fig. 8. Channel object parameters used in Petrel™ facies modelling. Shown are an areal view of the angle for channel direction, the definitions of wavelength and amplitude of a channel and an intersection view of the channel width and thickness. In addition, the fraction of channels compared to the matrix or the total number of channels present must be given.

step-wise if the reservoir architectures can be guided by observations during the ongoing CO_2 injection and consecutive monitoring. In the early stages, however, the reservoir model is constrained by the limited geological knowledge present at the time of construction. The first (pre-drilling) model relied mainly on the conceptual models of the sedimentological architecture of the Stuttgart Formation given by Beutler and Häusser (1982) and Beutler (2002) (see Förster et al., 2006). As the Ketzin project proceeded, further data became available which was assimilated into the model and enabled further refinement. For example, the 3D seismic data facilitated enabled a first update of the structural model by adding the interpreted surfaces of top and bottom of the Stuttgart Formation. In addition, the new boreholes in Ketzin supplied the true channel sand thicknesses at the injection site which form an important input to the stochastic facies modelling.

The seismic survey covers an area of about 12 km^2 (Juhlin et al., 2007). In order to allow for setting adequate boundary condition for the dynamic simulations, the reservoir model was extended to a rectangular area of 25 km^2. Thus, the structural interpretation of the horizon surfaces of the Stuttgart Formation was extrapolated using the topography of the seismic K2 horizon as trend horizon (Fig. 1). Based on the structural interpretation, a uniform mean thickness of 74 m was assumed for the Stuttgart Formation. Regarding the grid used in the geological modelling, the upper 37 m of the Stuttgart Formation where the main CO_2 flow is expected was gridded with a vertical resolution of half a metre. For the lower 37 m a vertical grid resolution of 1 m was chosen, whereas the horizontal grid cell dimensions are a uniform 20 m × 20 m for the entire model.

In the following, the data included in the facies and petrophysical modelling of the Ketzin baseline reservoir model is presented in more detail.

4.1. Facies modelling

It should be pointed out that the geometry of the sinuous channels produced by the geostatistical object modelling should not be regarded as a rendering of individual river channels at a certain point in time. Rather, the objects represent the cumulative deposition from fluvial processes within a channel belt over some time interval, and therefore are composite features with according internal heterogeneity originating from the deposition of point-bars, bottom sand bars, abandoned channel fills and discontinuous oxbow lakes. This system was addressed in a secondary step, in which spatial property variations were assigned within the channel belt.

4.1.1. Available data

Model input data included borehole-derived data such as the vertical distribution of channel facies, non-channel facies and further spatial-related data such as the horizontal distribution of properties based on analogue data, seismic data, or data from other studies. The latter includes information on the expected orientation and sinuosity of channels (Fig. 8), as well as information on the expected range of undulations of the sand channel and the likely variation of sand channel thickness and width.

4.1.2. Choice of facies and N/G-ratio

One important parameter for the facies model is the value for proportions of facies types present. For the Ketzin site, we considered two main facies types: channel sand facies and floodplain facies. The N/G-ratios determined from the boreholes in the larger Ketzin area (Fig. 4) display a remarkable heterogeneity, reflecting a spatial variability of channel density and stacking patterns. Thus, the question arises of what the characteristic fraction for the scale of

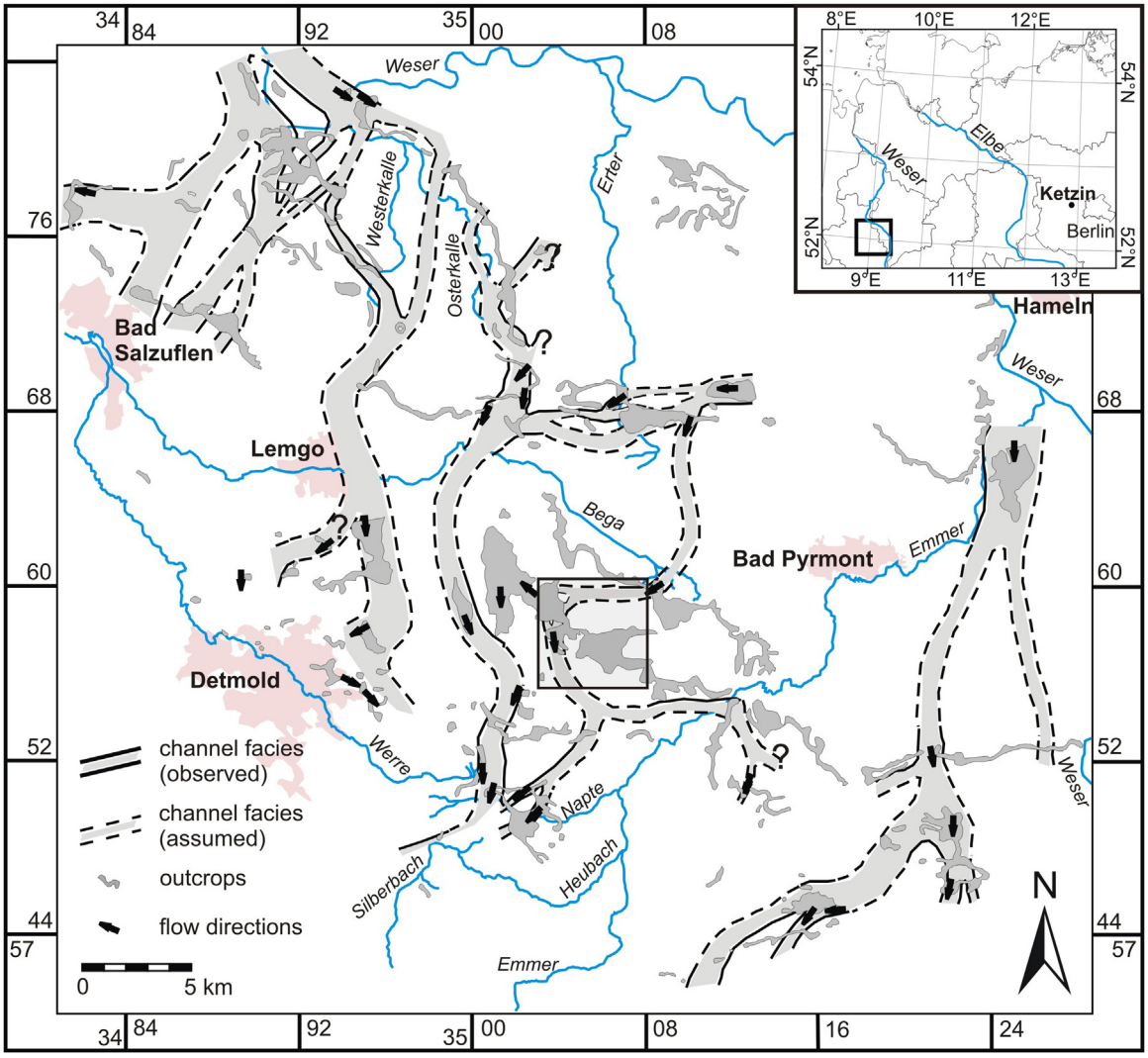

Fig. 9. Map showing the interpretation of the connectivity in the Stuttgart sand stringers based on scattered outcrop information and transport directions (Weserbergland; modified from Kruck and Wolf, 1975). Coordinate System: Gauß-Krüger (Rauenberg). Inlet map showing the positioning of the study areas of Weserbergland and Ketzin. The black square in the main map indicates the size of the Ketzin model domain area for comparison.

the reservoir model is. The interpretation from the detailed borehole data from the Ketzin site (Ktzi-200, Ktzi-201, and Ktzi-202) in a fairly limited area (maximum extent 110 m) may represent a biased sampling in comparison with the whole 5 km × 5 km reservoir model, as all drilling positions are located very close together. With the lack of spatial information and the intention of keeping the model simple, a constant ratio of 0.33 for the N/G was chosen for the whole model (Table 2), representing the mean value of all boreholes shown in Fig. 4.

4.1.3. Channel belt properties

For the Stuttgart Formation it is assumed that the regional trend of the deposits being shed from the Scandinavian Shield towards the south, i.e. N–S. Due to the assumed meandering nature of the individual fluvial channel, the current direction indications may deviate locally from the general channel belt orientation. The seismic spectral analysis data is very qualitative, but in general agreement with the assumption about the expected channel belt direction (Fig. 7). Only from one borehole, the Ktzi-201 borehole, data about the local current direction is available which is not in conflict with the general channel belt modelling assumptions. The mean channel belt orientation was set to 350 ± 10° (Table 2). Values for sinuosity (amplitude and wavelength), describing the channel belt geometry, were initially estimated from published data. Fig. 9 shows a possible channel distribution pattern based on outcrops of the Stuttgart Formation in northern Germany (Weser- und Osnabrücker Bergland). The sinuosity of the respective channels shows some variability on the km-scale: channel belt amplitudes and wavelengths range from 2 to 10 km and 5 to 10 km, respectively. However, these values are less well-supported by literature, as examples are rare. Wurster (1964) derived widths of individual fluvial channels that are in the order of several tens to several hundreds of metres; the derived mean channel-belt widths were estimated to amount to 1–2 km. Kruck and Wolff (1975) estimated channel belt widths of up to 4 km. The seismic data from Ketzin indicates similar trends; the estimated channel belt amplitudes and wavelengths based on the spectral decomposition (Fig. 7) are probably in the order of 1.5–3 km and 4–6 km if we extrapolate the course of the detected possible channel belt geometry. Based on the core data information on sand thickness and the correlation with the channel belt width as given in literature, and also looking at the seismic-data evaluation, the channel width was chosen according to Table 2. The minimum channel belt width of 600 m used for the modelling ignores the smaller width indication shown

Table 2
Input parameters used in (a) facies and (b) petrophysical modelling.

	Min.	Mean	Max.
(a) Parameter and values used in facies modelling			
N/G ratio		0.33	
Channel direction	340°	350°	360°
Channel amplitude	1 km	1.75 km	3 km
Channel wavelength	2 km	5.5 km	10 km
Channel width	600 m	900 m	2500 m
Channel thickness	1 m	4 m	10 m

	Min.	Max.	Vertical	Comments
(b) Parameter and values used in petrophysical modelling				
Total porosity channel facies	0.08	0.32		Allowed output range
Effective porosity channel facies	0.02	0.26		Collocated co-Kriging with total porosity using a correlation coefficient of 0.8
Total porosity floodplain facies	0.08	0.28		Allowed output range
Effective porosity floodplain facies	0.01	0.24		Collocated co-Kriging with total porosity using a correlation coefficient of 0.8
Anisotropy range	400 m	800 m	2 m	Variogram input
Anisotropy azimuth				
Permeability channel facies (mD)	$1{,}316{,}200 \times PHIT^{6.1}$			
Permeability floodplain facies (mD)	$187{,}350 \times PHIT^{6.8}$			
Permeability anisotropy	1 m grid size: ca. 0.5 ½ m grid size: ca. 0.4			Depends on grid size

by e.g. Kruck and Wolff (1975) since they could be based on their capture of deposits from individual fluvial channels, whereas the model produced here aims at reflecting the channel belt geometry.

The pre-drilling model was set-up using the FLUVSIM code (Deutsch and Tran, 2002) to illustrate the distribution of floodplain facies and channel facies (see Förster et al., 2006). The next model version represented a first reservoir model and used the facies simulation package of the commercial software Petrel, capable of handling all map, fault, well-log, and core data. However, the updated facies modelling of fluvial systems is based on similar principles as already used in the initial FLUVSIM model.

4.2. Modelling of petrophysical properties

The petrophysical properties included in the model are total porosity, effective porosity, and permeability. Although effective porosity is the parameter directly used in the dynamic modelling of the reservoir, we decided to model the distribution of total porosity as the first step. Total porosity has the advantage that it is the only parameter which can be derived from both well-log and core data, enabling us to establish a calibrated porosity log. In a second step, the distribution of effective porosity was modelled using co-simulation with total porosity. Finally, permeability was calculated from the total porosity using a modelled, site-specific porosity–permeability relationship based on the available core data.

At Ketzin, a comprehensive logging programme was performed consisting of routine well logging for all three wells and an enhanced logging programme for one single well (the CO_2 injection well Ktzi-201) that recorded nuclear-magnetic resonance (NMR) and borehole-resistivity images for reservoir characterization (Norden et al., 2010). For two Ketzin wells (Ktzi-200 and Ktzi-201), the complete Stuttgart Formation was cored and core samples measured for mineralogy (XRD), helium porosity, nitrogen permeability, and brine permeability at different pressure conditions. Based on the core control, an elemental log analysis model was established for all three wells and a porosity model determined. The determined porosity and permeability values range from 5 to >35% and 0.02 to >5000 mD, respectively (Norden et al., 2010). The results of the derived porosity data (both, effective and total porosity) of this integrated core-log analysis were screened for exceptional values and cross-checked with the technical and lithological data using the borehole descriptions. Thus, data interpreted at borehole breakouts and coal layers was excluded from the dataset in order to retain only data belonging to the two facies considered in the reservoir model. For each facies the data was analyzed for the distribution shown as histograms. Comparing core and combined core-log evaluated total porosity and permeability for the channel sandstones, Fig. 10 highlights a general good agreement. The QQ-plots for comparing the distributions of the core and log-based properties show that the distributions have a different shape for porosity values <20%, whereas for porosity values >20% the data points systematically depart from the 45° line; reflecting that the core-based porosity distribution has some very high values compared to the log-based porosity distribution. The maximum values from the core measurements reach above 40%, which seems as an improbable high porosity, and these could be deemed invalid. In terms of permeability, for values <1 mD the variance of the log-based data is greater than the core-based data; for values in the range of 1–550 mD, the plot shows some curvature, reflecting different shapes of the population distribution. In the permeability range from 550 to 1800 mD, the two distributions are nearly identical. Finally, the extremely high permeability values measured on some core samples are not reflected by the log-based evaluation. In order to derive the input for a target distribution of a sequential Gaussian simulation (SGS) of the porosity model, frequency density plots (Fig. 11) were calculated from the upscaled (at grid cell resolution) logging data. The upscaling of the well-log data was

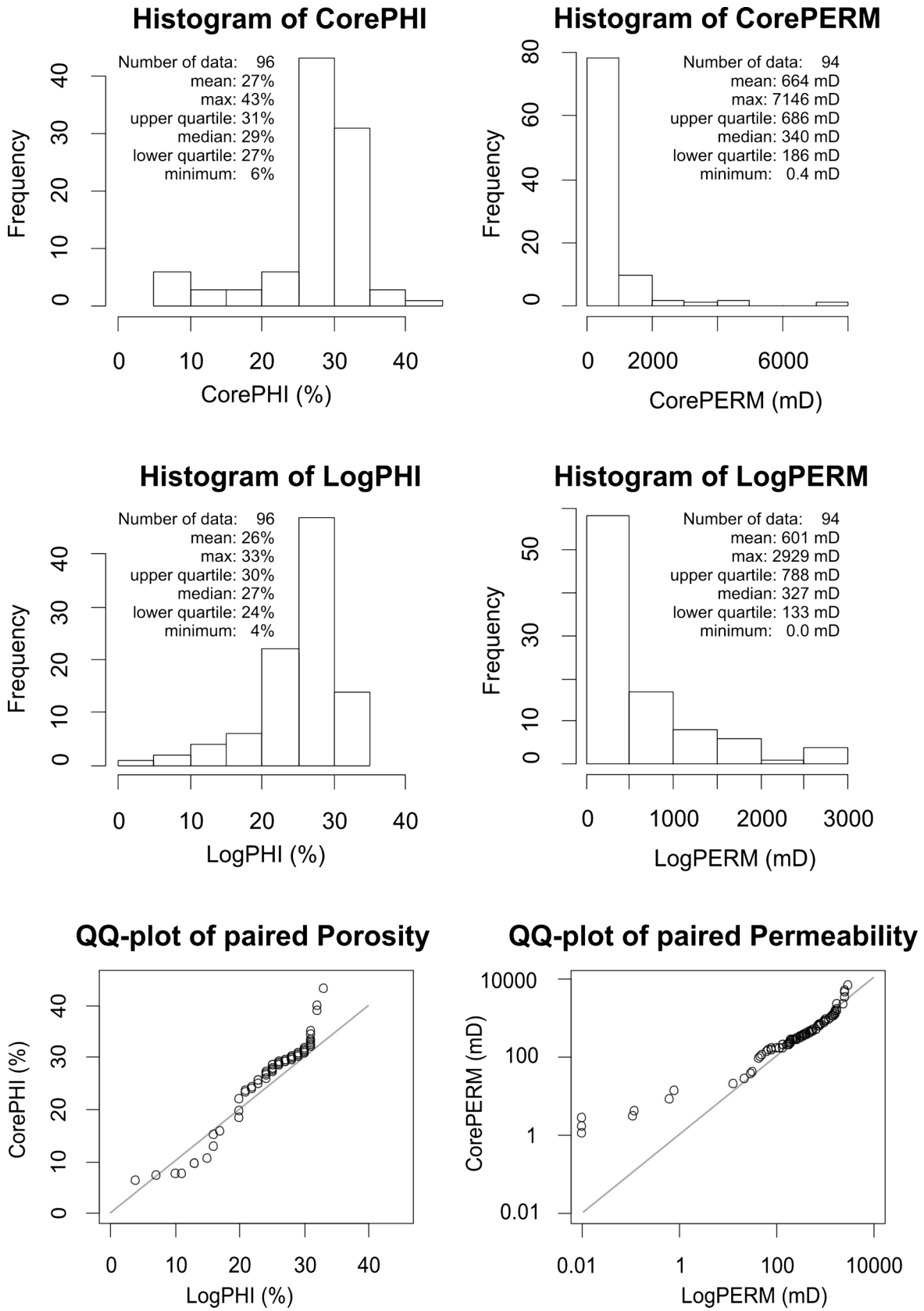

Fig. 10. Histograms and quantile–quantile (QQ)-plots of total porosity (PHI) and permeability (PERM) for both, core and log-evaluated data.
Source: Data from Norden et al. (2010).

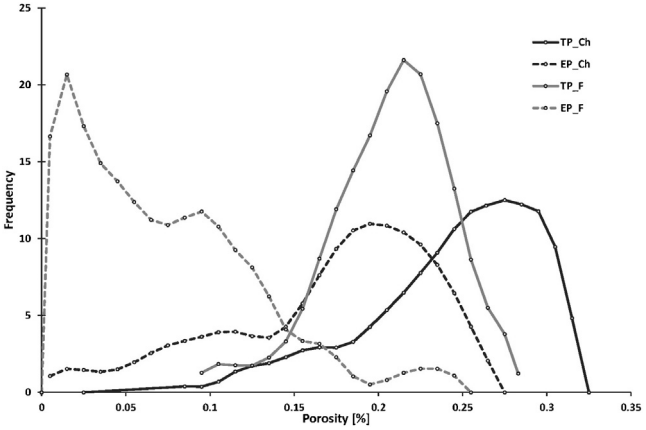

Fig. 11. Frequency-density plots of the total porosity (TP) and effective porosity (EP) distribution for both, the channel facies (Ch) and the floodplain facies (F) based on the core-log data of Norden et al. (2010).

performed by arithmetic averaging of the well log interpreted total and effective porosity into the grid with 0.50 m vertical scale. The effect is illustrated in Fig. 12 showing the original well-log interpreted effective porosity and the model-grid upscaled effective porosity used for the dynamic simulations. This transformation does not affect the distribution very much which can be seen by comparing histograms of the two data sets (Fig. 13).

The petrophysical anisotropy of individual facies is captured by defining variogram lengths and orientations for the SGS. As the spatial distribution pattern within the channel belt facies is not directly resolved by the Ketzin data, further assumptions were made with respect to anisotropy. For Ketzin, high-resolution seismic data (Kazemeini et al., 2009) give indications for a patchy distribution pattern (<500 m × 1000 m) of the permeable sandy reservoir rocks (see also Fig. 7). Such patterns were also shown by other studies (Carter, 2003). This information guided us in the decision about the values of the horizontal correlation range for the variograms used in the property modelling. For the vertical variogram correlation range, a segment of well data was analyzed. An interval from the upper part of the reservoir with sandy units was selected. The uppermost 40 m of the Stuttgart Formation was analyzed after the upscaling to grid size of 0.50 m. This shows that the upscaling has not changed the correlation structure significantly which can be modelled with a range of 3.2 m (Fig. 14a). In addition, the variogram for the porosity of only the channel facies is calculated and a variogram model with a range of 2.0 m is fitted (Fig. 14b). Based on this

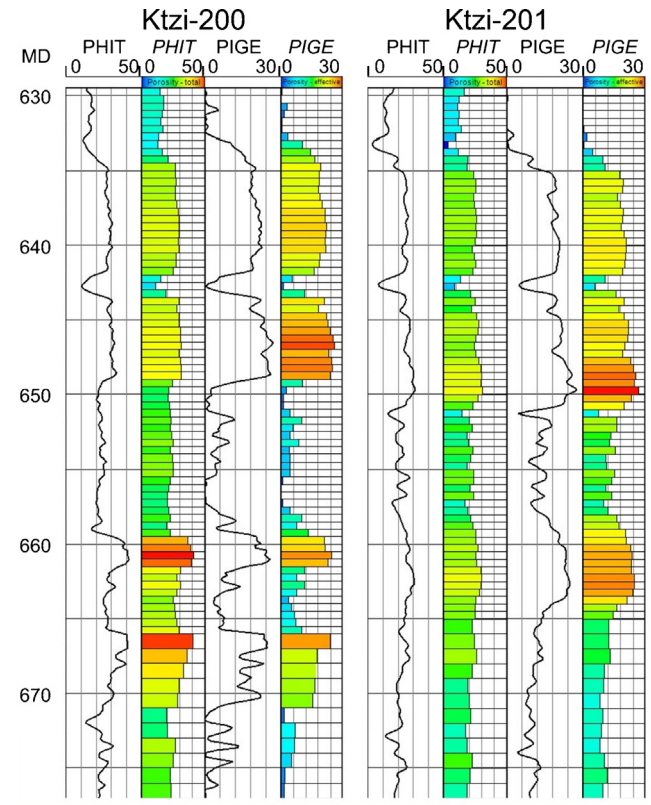

Fig. 12. Total and effective porosity from jointed core and well-log interpretation compared to upscaled cell properties used for dynamic simulations.

fit, the vertical variogram range of 2.0 m is used in the modelling of porosity heterogeneity within the channel facies.

Once the total porosity was simulated, the effective porosity was modelled for the two facies as being correlated with total porosity by using the collocated co-Kriging algorithm of Petrel. This algorithm uses co-Kriging with user input for a correlation coefficient between the two parameters (see Table 2).

Calculating permeability forms the last step in the petrophysical simulation. Permeability was estimated from log data on the basis of a nuclear magnetic-resonance open-hole logging measurement conducted in one borehole (Ktzi-201), supported by permeability measurements from core plugs (Norden et al., 2010). Furthermore, permeability was calculated using the Coates equation (Coates et al., 1991) based on an evaluation of the core-log integrated total

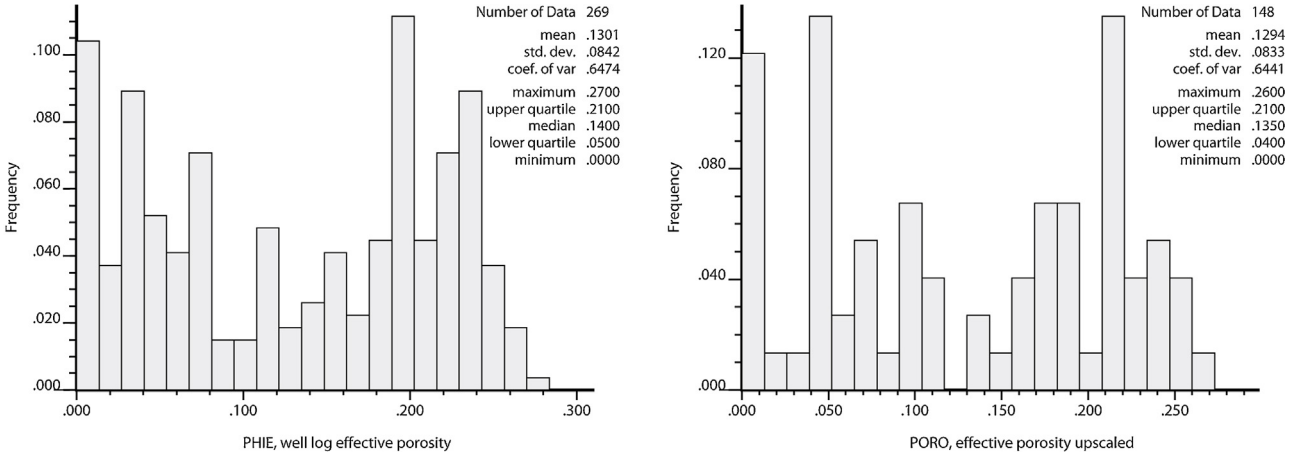

Fig. 13. Histograms for effective porosity for the upper 40 m of the reservoir from the well log data at resolution 0.15 m and for the grid upscaled porosity at 0.50 m resolution.

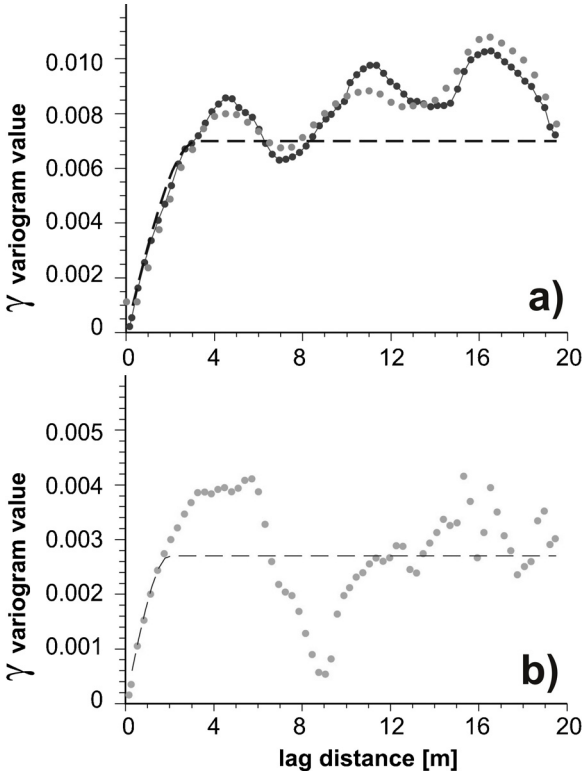

Fig. 14. (a) Variograms calculated from the well log data for the upper 40 m reservoir (dark grey points and line), and for the grid upscaled effective porosity (grey points), and the modelled variogram (dashed line). (b) Variogram calculated for the porosity log data only in the channel facies, resulting in a variogram model with a range of 2.0 m.

porosity volume. This allows the interpretation of the logging data in terms of porosity and permeability for the Ktzi-202 borehole, where no permeability measurements on cores were performed (Norden et al., 2010). Based on the integrated core plug and log data analysis, the porosity–permeability relationships shown in Fig. 14 was derived. These are believed to be representative for the horizontal permeability and are linked to the two different facies types. The channel sands have the highest permeability whereas the floodplain deposits are considered of generally lower quality, containing more clay resulting in a lower permeability for similar porosities.

To fully model the spatial distribution of permeability, vertical permeability and thus, the anisotropy of permeability needs to be considered. From the measured core data there is no clear trend observable as only a limited number of vertical permeabilities were determined and horizontal and vertical permeabilities were not measured on the same samples. Also no account was taken of the stratified bed boundaries which are relevant for the vertical permeability. In fact, anisotropy is very much depending on the grid size chosen in relation to the size scale of the heterogeneities in the rock. If a laminated rock with large permeability contrasts between the individual lamina is represented by a single block much larger than the lamina size in the vertical direction, a very high anisotropy can be expected. In order to investigate this phenomenon in the sandy facies, several 1-m core sections were chosen which were measured using a gamma-density core scanner. The density recordings at fine scale (every cm) were converted to porosity assuming mineral and brine densities of 2.64 and 1.152 g/cm^3, respectively. The porosity estimate was then converted to fluid permeability with the determined porosity–permeability equation for the channel facies (Figs. 15 and 16). Anisotropy of permeability was calculated as the ratio between the harmonic and the arithmetic averages of permeability. For the shown cores of the Ktzi-200 borehole, anisotropy is less relevant due to the more uniformly distributed permeability ranges. In contrast, for the core of the Ktzi-201 borehole shown in Fig. 16, which includes the highest contrast in density (permeability) changes over the core metre, anisotropy amounts to 0.43 and 0.56 for a 0.5 m and a 1.0 m interval, respectively. In order to account for permeability contrasts that are not resolved in the core scanning and their effect on the effective anisotropy on the reservoir scale, the value of 0.4 was chosen for the model. Table 2 summarizes the parameters and values used in the facies and petrophysical modelling.

5. Results

Stochastic modelling produces multiple possible realizations for facies architecture and petrophysical properties for the model

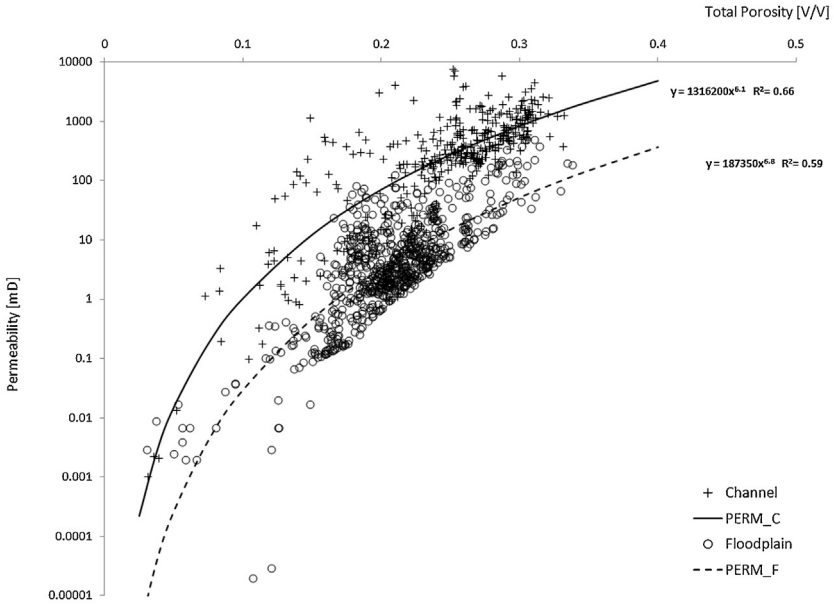

Fig. 15. Porosity–permeability relationship from integrated analysis of core and borehole logging measurements.

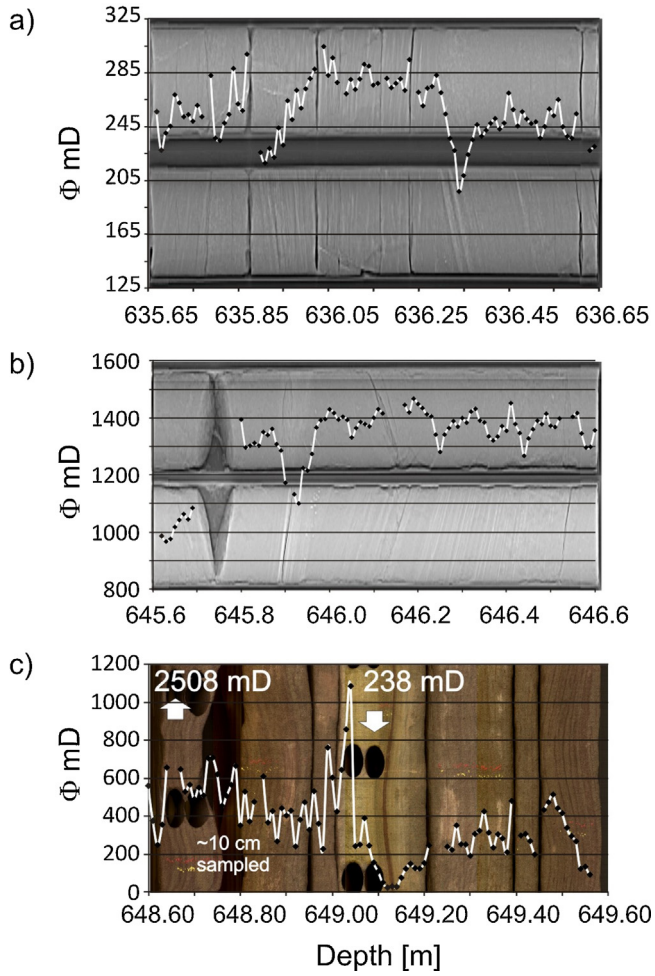

Fig. 16. Estimation of permeability from density core logging to evaluate anisotropy. Shown are three cores with the calculated permeabilities based on porosity estimates using the measured core density. In the background, CT images of the core (a and b) and a rolled core image (c) are shown. (a and b) Cores 200-13_1 and 200-16_2 (c. Fig. 6) with an anisotropy of 0.99 (1 m) and 0.98 (1/2 m), (c) core 201-11_2 from the CO_2 Ktzi 201/2007 borehole with an anisotropy of 0.43 (1 m)–0.56 (1 m). In addition, results from core plug analysis are plotted.

constraints used as input to the model. Examples are shown in Figs. 17 and 18. In certain areas, channels are stacked and yield higher total channel thicknesses than given as maximum values in Table 2 (highlighted by ellipses in Fig. 17). In addition, the section view of the model (Fig. 17) visualizes the N/G-relation of channel to floodplain facies in general. Fig. 18 shows the distribution of the channel belt facies for three other realizations along constant depth intervals (approximately 5 and 10 m below Top Stuttgart, hitting the drilled upper channel sandstone at the Ketzin boreholes). Based on over 60 simulations of the facies distribution, it can be concluded that it is very likely that the channel bodies of the drilled boreholes are related to the same channel or to two channels which are connected. In all realizations, the channel sandstones of the Ktzi-200 and Ktzi-201 boreholes are situated in the same channel belt system. However, in some realizations floodplain facies is present between the Ktzi-200/Ktzi-201 boreholes and the Ktzi-202 borehole. In terms of porosity, Fig. 19 illustrates some possible scenarios. Plotted are average porosity maps for the uppermost 20 m of the model, in the depth range where also the channel sandstone was encountered in the Ketzin boreholes. Based on the respective facies realization, a patchy distribution of the mean total porosity is observable, showing maximum values along the simulated channel ways. The facies-dependency of the hydraulic properties becomes even more obvious in the distribution of the effective porosity.

In order to show the consequences from the geological model of the fluvial depositional system for the flow simulation studies, one result was extracted for illustrating the effect of directionality of the sand-bodies (Fig. 20). The CO_2 is entering the reservoir at several levels, for which the direction of migration can vary due to the architecture of the permeable sands. This variability in the migration pattern must of course be considered in the monitoring strategy.

6. Discussion

Considering the sparse and potentially biased input data available, the reservoir model will not be able to reflect the "true" in situ condition, but only a probabilistic version honouring the present data and the geometry parameters used for the modelling. As all models represent a limited reproduction of the reality, the first question to ask is if the model conforms to the geological input data, thus, if the geological model is able to represent the characteristic conditions of the subsurface in principle. The architecture of the model is triggered to a large extent by the simulated facies distribution. Similar conditions as assumed for Ketzin are for example found in the Miocene Huesca fluvial fan in Spain (Donselaar and Overeem, 2008). This meandering river system shows lateral amalgamation and vertical stacked channels with an N/G-ratio of about 40%. The channels occur in 1–1.5 km wide meander belts occupying paleo valleys (Donselaar and Overeem, 2008). The relatively moderate sinuosity of the channel belts is similar to the expected situation in Ketzin (see Donselaar and Overeem, 2008: Fig. 4). Channel belt amplitudes are on the order of 300–500 m. Bank-full depth (channel thickness) are interpreted to reach 4 m, also similar to Ketzin. Whereas at the Spanish site well exposed outcrops allow a detailed characterization of the fluvial system, much of the interpretation of the Ketzin site relies on general assumptions and could not finally be resolved by the available borehole data. For example, the sandy deposits of Ketzin do not show a classical point-bar sequence with clear fining upward trends. Thus, channel facies may be misinterpreted at Ketzin. However, the lack of fining trends could also be due to the overall homogeneity of the available sediment as almost only fine-grains are present in the grain-size spectrum. This might be due to the transport distance and history.

Another possible example of a facies analogue to the sandstones of the Stuttgart Formation is described by Hornung and Aigner (1999) from the Upper Triassic Stubensandstein in southwest Germany, which could be interpreted as a system of channel elements in a very similar setting compared to Ketzin. They report channel bodies with thicknesses of 1–10 m and a channel width of several hundred metres (Hornung and Aigner, 1999). The w/t ratio is estimated to amount to 10–50:1 (Hornung and Aigner, 2002). According to Hornung and Aigner (2002), the higher ranges of the mentioned w/t ratios are associated with bed-load dominated meandering fluvial style. In addition, the petrophysical characteristics of the bed-load channel sandstone elements presented by Hornung and Aigner (1999) are comparable with the characteristics observed in the Ketzin channel sandstone, except for the fact that the sandstones of the Stubensandstein are coarser grained. In detail, the gamma-ray reading does not show any change in intensity over the sandstone interval (as it is often discussed to be typically for channel point bar deposits showing a fining-upward sequence, see e.g. Rider, 2000), whereas the permeability shows higher values at or just above the base of the sandy sequence. A similar pattern could be recognized in the Ketzin data as well (cf. Fig. 5). Although we do not have knowledge about the precise geometrical distribution of the petrophysical properties at Ketzin, we may assume that

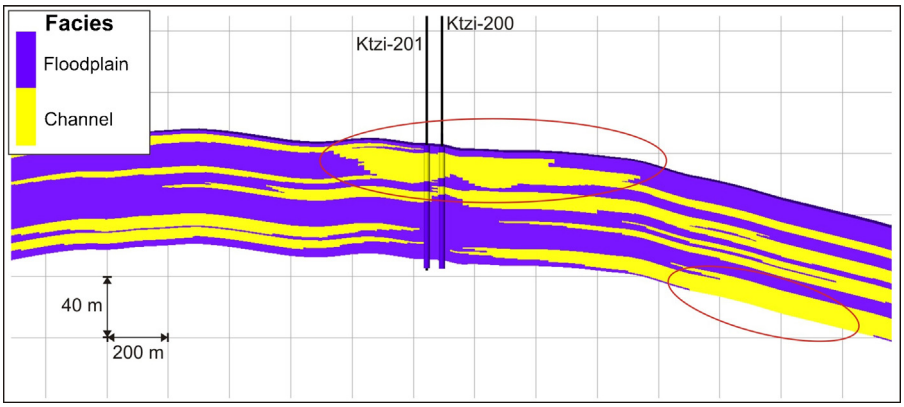

Fig. 17. Section view of the reservoir model (realization 04_27, section along 5,820,000 N, looking from south). Different channel shapes and stacked channel geometries could be observed. The ellipses show areas of stacked channels, resulting in high channel thicknesses. Vertical exaggeration: 5 times.

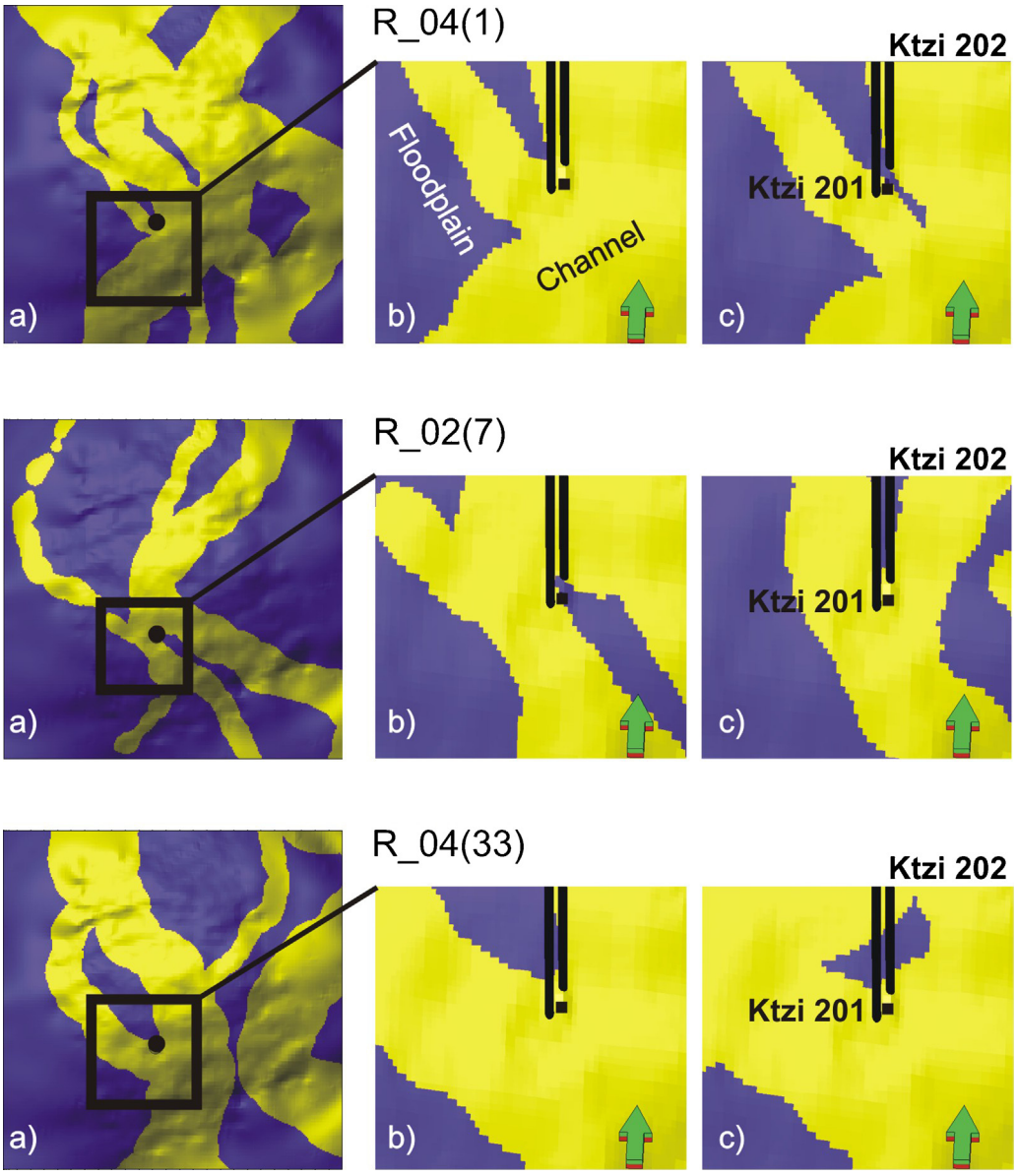

Fig. 18. Facies distribution of three different realizations [from top to bottom: R_04(1), R_02(7), and R_04(33)]: (a) for the entire model domain (5 km × 5 km) at a depth level approximately 5 m below top of Stuttgart Formation; (b) zoom-in for the same depth level as in (a) showing the well paths of the Ktzi-201 and Ktzi-202 boreholes and the positioning of the Ktzi-200 borehole (black square) in relation to the channel facies (the distance between Ktzi-201 and Ktzi-202 amounts to about 110 m); (c) for the same area as in (b) but approximately 10 m below top of Stuttgart Formation. The black dot in subfigure (a) denotes the location of the Ketzin injection site.

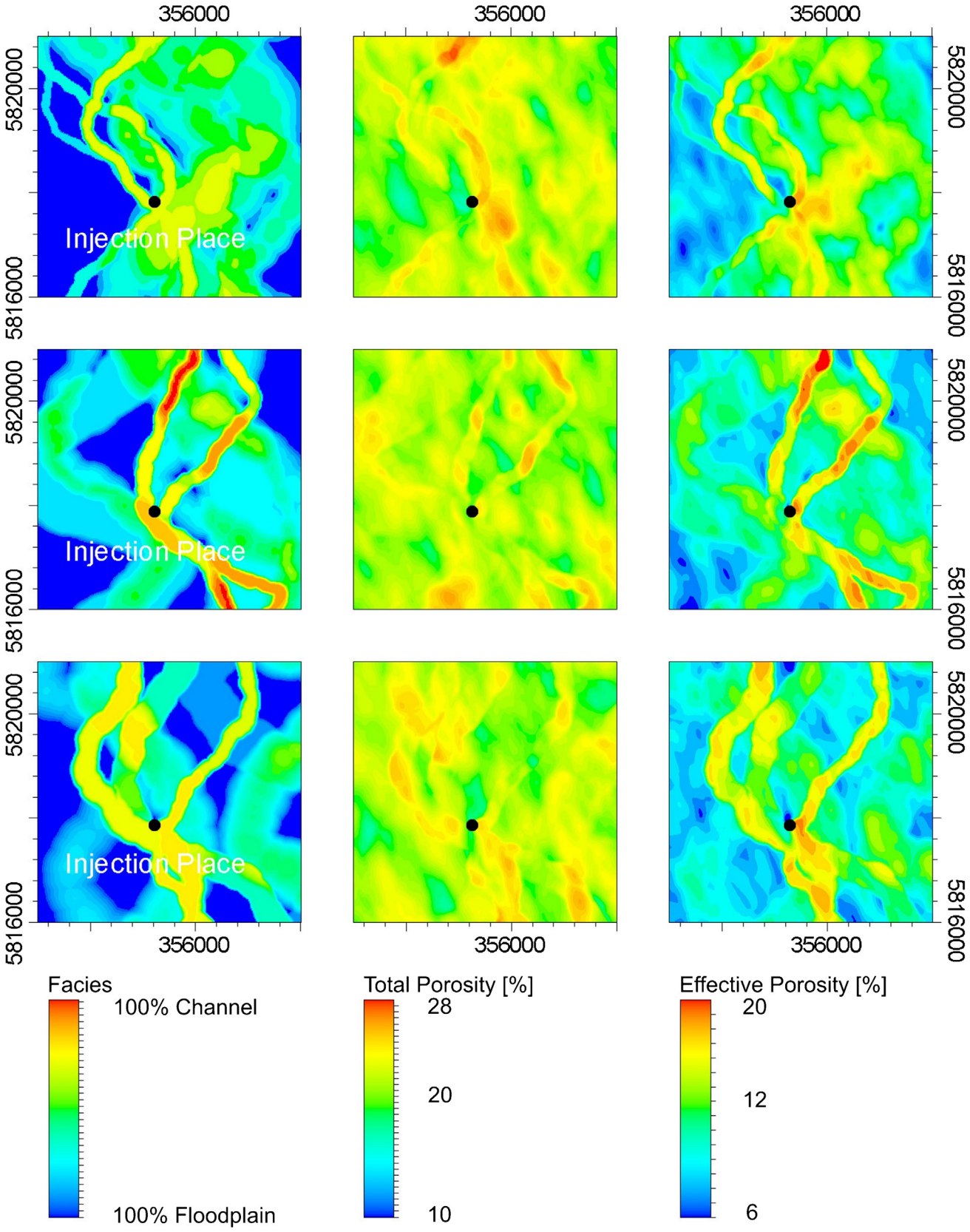

Fig. 19. Average facies and porosity maps of the uppermost 20 m of the model for three different facies models. Plotted are mean facies distribution (left panel), average total porosity (middle panel), and effective porosity (right panel). The location of the Ketzin injection facility is indicated by a black dot.

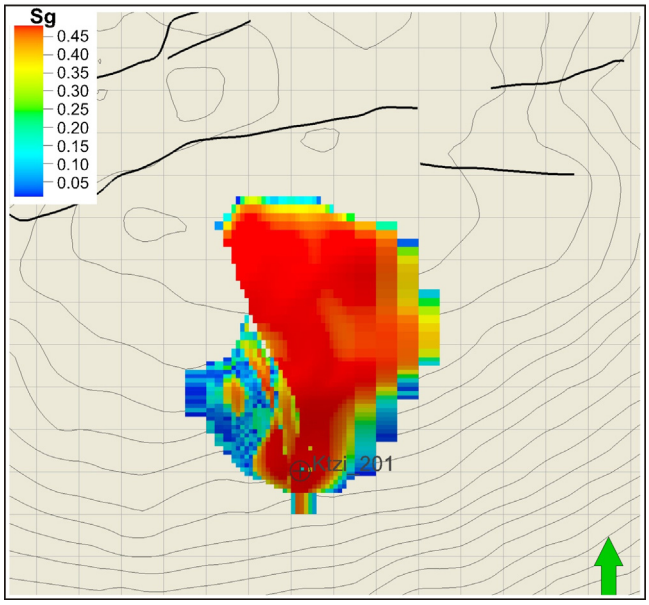

Fig. 20. Map view of the distribution of free-phase CO_2 saturation (Sg) in a selected realization of the Ketzin reservoir model. Flow simulation of injection into the well Ktzi-201 showing the uneven distribution of CO_2 following the direction of the fluvial sand-bodies in the reservoir model. This map view is looking down onto several layers of migrating CO_2 which has entered the reservoir at different levels according to the architecture of the permeable sands. The contours for the reservoir map are shown as underlay, and the major faults on the crest of the structure are indicated. The scale is indicated by the meshing grid (200 m × 200 m).

the data presented by Hornung and Aigner (1999, 2002), which are based on outcrop data, may be an analogue to Ketzin. Seismic methods seem to be able to illustrate the distribution, size, and range of point-bar deposits if their acoustic properties and their thickness are sufficient to produce an adequate seismic response. For the Ketzin data, spectral decomposition and amplitude analysis give vague indications for the sandy reservoir distribution. Another example is presented by Carter (2003) from the Widuri field of the Java Sea, showing the patchiness of porous sands (Fig. 21). Although the channel belt geometry could not be seen very clearly, the same

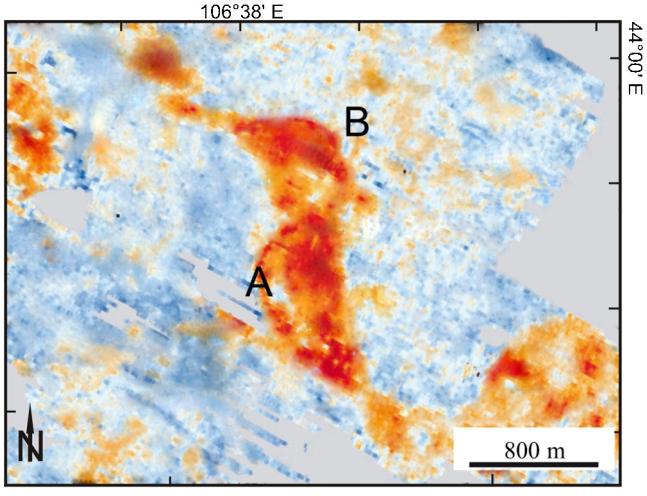

Fig. 21. Amplitude image from the Widuri Field, Java Sea. The red colouring indicates higher amplitudes which are interpreted to represent high-porosity sandstone bodies (for example between A and B; modified from Carter, 2003). (For interpretation of the references to colour in this figure legend, the reader is referred to the web version of this article.)

order of sinuosity of the sandstone bodies that are assumed for Ketzin could be inferred from Fig. 21.

The exact geometrical distribution of facies and related properties is also related to the choice of the input data. The N/G-ratios presented in Fig. 4 shows some extreme values for the Ug Ktzi 163/69 and the TB P 13/73 boreholes (0.64 and 0.07, respectively). Most boreholes, except the CO_2 Ktzi 200–202 boreholes, show sandy intervals at the bottom or middle of the Stuttgart Formation, whereas the newer Ketzin boreholes show the reverse trend at the Ketzin site (Fig. 4). Therefore, the actual distribution of the N/G-ratio in the whole model domain is expected to be variable and remains uncertain. Up to now we could not link reliable seismic attribute data (e.g. from spectral decomposition of certain depth zones) with vertical N–G ratio profiles of boreholes. Any changes of the N/G-distribution pattern will of course influence the modelled facies geometry, i.e. the distribution and the thickness of the channels.

The dynamic modelling of the CO_2 migration during the injection phase shows that the modelling of a fluvial system is probably most challenging when it comes to its consequences for the CO_2 distribution. The combination of high permeability contrasts between sand bodies and adjacent channel-fill, the directionality of the original channels, and the tendency for the CO_2 to seek the highest layers due to the gravity override, is creating an extreme variability in the CO_2 distribution by only slight changes in the geological model. In other geological settings of e.g. marine near-shore deposits, this effect of interaction would be different and maybe make the CO_2 distribution pattern more resilient to architectural changes. For the well-known Sleipner case, there is still some uncertainty about the depositional environment (Chadwick et al., 2004), but the general architecture is a fairly homogeneous sandy lithology with extremely high permeability, although with some thin (discontinuous?) shale layers influencing the near-well behaviour of the filling process. The larger scale behaviour of this site is therefore totally dominated by the topology of the bottom-surface of the caprock, where even small topographical differences direct the CO_2 migration. This is in marked contrast to a fluvial system like displayed in the Ketzin site, where compartmentalization of the reservoir could determine more directly where the CO_2 migrates.

In terms of the petrophysical parameterization, porosity and permeability data for the Stuttgart Formation available in the literature includes reservoir rocks only. Wolfgramm et al. (2008) gave a compilation of reservoir properties of Mesozoic sandstones of the Northeast German Basin. For the Stuttgart Formation, petrophysical and petrographical data from only three boreholes, all located more than 100 km northwest to northeast of Ketzin, are documented. The analyzed sandstones show mainly pore spaces of less than 5 μm and a high variability of sorting, ranging from good to very poor, indicating a very variable quality of the reservoir properties (Wolfgramm et al., 2008). Rockel and Schneider (1999) reports reservoir permeabilities determined at geothermal project sites from the same locations as Wolfgramm et al. (2008) to amount between 20 and 150 mD. They state that it was not possible to utilize channel sandstones for geothermal purposes because they were not encountered at these sites. Therefore, it remains an open question, how representative the available petrophysical data for the lithological heterogeneous Stuttgart Formation is. In Ketzin, reservoir permeabilities deduced from hydraulic tests indicate permeabilities between 50 and 100 mD (Wiese et al., 2010); significantly lower (about one order of magnitude) compared to that from core and log analysis. Most likely, further structural features like cemented fractures or sedimentary heterogeneities are responsible for the lowered field permeability as it was observed in the hydraulic tests (Wiese et al., 2010) (cf. Fig. 6a). In order to consider these results in the modelling, a simple correction factor, reducing the permeability in the model, is used until now, as it

has been shown to improve the history match of injection pressure (Pamukcu et al., 2011).

We must be aware that the geological model might honour the general setting characteristics, but it is not representing the details correctly. Therefore, the different types of mismatches discovered during the continued monitoring and development of the site, serves to focus our attention on the subsurface features which ought to be observed further and included in the model update. As an example, the mentioned differences in derived permeabilities indicate either lateral limitation of the reservoir layer, near-well skin effects, or some unrecognized features of fracturation/cementation, all of which would tend to reduce the larger-scale permeability observed in the well tests and in the pressure history matching exercise.

7. Conclusions

In order to simulate realistic scenarios for the reservoir characterization, very much is depending on the assumed depositional concept. Based on the available information, a fluvial environment consisting of channel and floodplain depositional facies is assumed at Ketzin. Analysis of literature data, borehole data, and seismic data provide estimates for the dimensions and architectural stacking of the sand bodies. Because the uncertainty related to establishing firm input parameters for fluvial systems is considerable as shown by Miall (2006) and Gibling (2006), the combination and joint interpretation of the available data becomes most important in order to enable the development of a coherent facies and reservoir model.

This paper describes a typical modelling work flow for determining input parameters for setting up a geo-model that can be used for studies of dynamic reservoir behaviour. The initial model (before the CO2 Ktzi boreholes were drilled) was constructed using regional geological interpretations, wells outside the immediate site area and conceptual ideas. This model served the purpose of presenting possible large scale migrations patterns for the injected CO_2, and for capturing the general structure. When the interpretation of the 3-D seismic data and the information from the three CO2 Ktzi drillings was incorporated to the model, a refinement of the input parameters helped narrowing the uncertainty related to the model architecture. As more data from the monitoring during injection operation become available, this refinement will progress further, allowing also to place deterministic elements into the model.

Building reservoir models involves multi-disciplinary input and the compilation of very different data and data quality. Depending on the degree of exploration and knowledge, on one hand, and on the overall purpose of the reservoir model, on the other hand, the model design needs to be adapted. For Ketzin, the presented reservoir model was used to successfully initiate the injection of CO_2 and to calculate the CO_2 arrival times for one of two observation wells. As soon as monitoring data become available, the static geological model needs to be updated to include the structural information which can be obtained from e.g. the time-lapse seismics. For example, Ivanova et al. (2012) presented first monitoring and volumetric estimates based on 4D seismic data. Again, the comparison of monitoring data and the simulated extension of the migrating CO_2 will direct attention to the question of resolution of the seismic imaging, and therefore to the uncertainty in any quantification of volumes from the seismic observations. Static and dynamic reservoir simulations together with new site data from seismic and electrical monitoring as well as the expected data from a new borehole, drilled into the storage formation in 2012, will help to improve the seismic and geological interpretation and the geological static model in return.

Acknowledgements

The research described in this paper is funded by the European Commission (Sixth and Seventh Framework Program), two German Ministries—the Federal Ministry of Economics and Technology and the Federal Ministry of Education and Research—and industrial partners (VNG, Vattenfall, RWE, Statoil, Dillinger Hüttenwerke, Saarstahl, OMV) which are thanked for supporting this study (www.co2ketzin.de). One anonymous reviewer and especially Jan Tveranger are thanked for their valuable comments. This is Geotechnologien paper number GEOTECH-1999.

References

Aigner, T., Bachmann, G.H., 1992. Sequence-stratigraphic framework of the German Triassic. Sedimentary Geology 80, 115–135.

Beutler, G., 2002. Keuper-Mächtigkeit und Lithofazies des Schilfsandsteins. In: Stackebrandt, W., Manhenke, V. (Eds.), Atlas zur Geologie von Brandenburg im Maßstab 1:1,000,000. Kleinmachnow, Landesamt für Geowissenschaften und Rohstoffe Brandenburg, Germany, pp. 62–63.

Beutler, G., Häusser, I., 1982. Über den Schilfsandstein in der DDR. Zeitschrift für Geologische Wissenschaften 10, 511–525.

Beutler, G., Tessin, R., 2005. Der Keuper im Norddeutschen Becken. In: Beutler, G. (Ed.), Stratigraphie von Deutschland IV, vol. 253. Keuper, Cour. Forsch.-Inst, Senckenberg, pp. 134–150.

Beutler, G., Hauschke, N., Nitsch, E., 1999. Faziesentwicklung des Keupers im Germanischen Becken. In: Hauschke, N., Wilde, V. (Eds.), Trias – Eine ganz andere Welt. Mitteleuropa im frühen Erdmittelalter, Pfeil, München, pp. 129–174.

Bridge, J.S., Mackey, S.D., 1993. A theoretical study of fluvial sandstone body dimensions. In: Flint, S.S., Bryant, I.D. (Eds.), Geological Modeling of Hydrocarbon Reservoirs: International Association of Sedimentologists, vol. 15. Special Publication, Utrecht, The Netherlands, pp. 213–236.

Bridge, J.S., Tye, R.S., 2000. Interpreting the dimensions of ancient fluvial channel bars, channels, and channel belts from wireline-logs and cores. AAPG Bulletin 84 (8), 1205–1228.

Carter, D.C., 2003. 3-D seismic geomorphology: insights into fluvial reservoir deposition and performance, Widuri field, Java Sea. AAPG Bulletin 87 (6), 909–934.

Chadwick, R.A., Zweigel, P., Gregersen, U., Kirby, G.A., Holloway, S., Johannessen, P.N., 2004. Geological reservoir characterization of a CO_2 storage site: the Utsira Sand, Sleipner, Northern North Sea. Energy 29, 1371–1381.

Coates, G.R., Peveraro, R.C.A., Hardwick, A., Roberts, D., 1991. The magnetic resonance imaging log characterized by comparison with petrophysical properties and laboratory core data. In: Paper SPE 22723 Presented at the SPE Annual Technical Conference and Exhibition, Dallas, 6–9 October, http://dx.doi.org/10.2118/22723-MS.

Deutsch, C.V., Tran, T.T., 2002. FLUVSIM: a program for object-based stochastic modeling of fluvial depositional systems. Computers & Geosciences 28 (3), 525–535.

Donselaar, M.E., Overeem, I., 2008. Connectivity of fluvial point-bar deposits: an example from the Miocene Huesca fluvial fan, Ebro Basin, Spain. AAPG Bulletin 92 (9), 1109–1129.

Eigestad, G.T., Dahle, H.K., Hellevang, B., Riis, F., Johansen, W.T., Oian, E., 2009. Geological modeling and simulation of CO_2 injection in the Johansen formation. Computational Geosciences 13, 435–450.

Ethridge, F.G., 2011. Interpretation of ancient fluvial channel deposits: review and recommendations. From River to Rock Record: The Preservation of Fluvial Sediments and Their Subsequent Interpretation, vol. 97. SEPM Special Publication, pp. 9–35.

Förster, A., Norden, B., Zinck-Jørgensen, K., Frykman, P., Kulenkampff, J., Spangenberg, E., Erzinger, J., Zimmer, M., Kopp, J., Borm, G., Juhlin, C., Cosma, C.-G., Hurter, S., 2006. Baseline characterization of the CO_2SINK geological storage site at Ketzin, Germany. Environmental Geosciences 13 (3), 145–161.

Förster, A., Schöner, R., Förster, H.-J., Norden, B., Blaschke, A.-W., Luckert, J., Beutler, G., Gaupp, R., Rhede, D., 2010. Reservoir characterization of a CO_2 storage aquifer: the Upper Triassic Stuttgart Formation in the Northeast German Basin. Marine and Petroleum Geology 27 (10), 2156–2172.

Gibling, M.R., 2006. Width and thickness of fluvial channel bodies and valley fills in the geological record: a literature compilation and classification. Journal of Sedimentary Research 76, 731–770.

Harvey, R.D., Dillon, J.W., 1985. Maceral distributions in Illinois coals and their paleoenvironmental implications. International Journal of Coal Geology 5, 141–165.

Hornung, J., Aigner, T., 1999. Reservoir and aquifer characterization of fluvial architectural elements: Stubensandstein, Upper Triassic, southwest Germany. Sedimentary Geology 129, 215–280.

Hornung, J., Aigner, T., 2002. Reservoir architecture in a terminal alluvial plain: an outcrop analogue study (Upper Triassic, southern Germany). Part II: cyclicity, controls and models. Journal of Petroleum Geology 25 (2), 151–178.

Hoth, K., Rusbült, J., Zagora, K., Beer, H., Hartmann, O., 1993. Die tiefen Bohrungen im Zentralabschnitt der Mitteleuropäischen Senke – Dokumentation für den Zeitabschnitt 1962–1990. Schriftenreihe für Geowissenschaften 2, Gesellschaft für Geowissenschaften e.V. (i.G.), Berlin, 145 p.

Ivanova, A., Kashubin, A., Juhojuntti, N., Kummerow, J., Henninges, J., Juhlin, C., Lüth, S., Ivandic, M., 2012. Monitoring and volumetric estimation of

injected CO_2 using 4D seismic, petrophysical data, core measurements and well logging: a case study at Ketzin, Germany. Geophysical Prospecting, http://dx.doi.org/10.1111/j.1365-2478.2012.01045.x.

Johnson, J.W., 2009. Integrated modeling, monitoring, and site characterization to assess the isolation performance of geologic CO_2 storage: requirements, challenges, and methodology. Energy Procedia 1, 1855–1861.

Juhlin, C., Giese, R., Zinck-Jørgensen, K., Cosma, C., Kazemeini, H., Juhojuntti, N., Lüth, S., Norden, B., Förster, A., 2007. 3D baseline seismics at Ketzin, Germany: the CO_2SINK project. Geophysics 72 (5), B121–B132.

Kaufmann, O., Martin, T., 2008. 3D geological modelling from boreholes, cross-sections and geological maps application over former natural gas storages in coal mines. Computers & Geosciences 34, 278–290.

Kazemeini, S.H., Juhlin, C., Zinck-Jørgensen, K., Norden, B., 2009. Application of the continuous wavelet transform on seismic data for mapping of channel deposits and gas detection at the CO_2SINK site Ketzin, Germany. Geophysical Prospecting 57 (1), 111–123.

Kempka, T., Kühn, M., Class, H., Frykman, P., Kopp, A., Nielsen, C.M., Probst, P., 2010. Modelling of CO_2 arrival time at Ketzin – Part I. International Journal of Greenhouse Gas Control 4, 1007–1015.

Kopp, A., Probst, P., Class, H., Helmig, R., 2009. Estimation of CO_2 storage capacity coefficients in geologic formations. Energy Procedia 1, 2863–2870.

Kruck, W., Wolff, F., 1975. Ergebnisse einer Fazieskartierung im Schilfsandstein des Weserberglandes, vol. 44. Mitt. Geol.-Paläont. Inst. Univ. Hamburg, pp. 417–421.

Leclair, S., Bridge, J.S., 2001. Quantitative interpretation of sedimentary structures formed by river dunes. Journal of Sedimentary Research 71 (5), 713–716.

Lengler, U., De Lucia, M., Kühn, M., 2010. The impact of heterogeneity on the distribution of CO_2: numerical simulation of CO_2 storage at Ketzin. International Journal of Greenhouse Gas Control 4, 1016–1025, http://dx.doi.org/10.1016/j.ijggc.2010.07.004.

Martens, S., Kempka, T., Liebscher, A., Lüth, S., Möller, F., Myrttinen, A., Norden, B., Schmidt-Hattenberger, C., Zimmer, M., Kühn, M., Ketzin Group, 2012. Europe's longest-operating on-shore CO_2 storage site at Ketzin, Germany: a progress report after three years of injection. Environmental Earth Sciences, http://dx.doi.org/10.1007/s12665-012-1672-5.

Miall, A.D., 1996. The Geology of Fluvial Deposits. Springer, Berlin.

Miall, A.D., 2006. Reconstructing the architecture and sequence stratigraphy of the preserved fluvial record as a tool for reservoir development: a reality check. AAPG Bulletin 90 (7), 989–1002.

Norden, B., Förster, A., Vu-Hoang, D., Marcelis, F., Springer, N., Le Nir, I., 2010. Lithological and petrophysical core-log interpretation in CO_2SINK the European CO_2 onshore research storage and verification project. SPE Reservoir Evaluation & Engineering 13 (2), 179–192.

Pamukcu, Y., Hurter, S., Frykman, P., Moeller, F., 2011. Dynamic simulation and history matching at Ketzin (CO_2SINK). Energy Procedia 4, 4433–4441, http://dx.doi.org/10.1016/j.egypro.2011.02.397.

Prevedel, B., Wohlgemuth, L., Legarth, B., Henninges, J., Schütt, H., Schmidt-Hattenberger, C., Norden, B., Förster, A., Hurter, S., 2009. The CO_2SINK boreholes for geological CO_2-storage testing. Energy Procedia 1 (1), 2087–2094.

Reinhardt, H.-G., 1993. Regionales Kartenwerk der Reflexionsseismik. VEB Geophysik Leipzig, Leipzig.

Ricken, W., Aigner, T., Jacobsen, B., 1998. Levee-crevasse deposits from the German Schilfsandstein. Neues Jahrbuch für Geologie und Paläontologie Mh, pp. 77–94.

Rider, M., 2000. The Geological Interpretation of Well Logs. Whittles Publishing, Caithness, Scotland, pp. 280.

Rockel, W., Schneider, H., 1999. Triassische Sandsteine als bedeutsame geothermische Nutzhorizonte. In: Hauschke, N., Wilde, V. (Eds.), Trias – Eine ganz andere Welt. Mitteleuropa im frühen Erdmittelalter, Pfeil, München, pp. 531–540.

Schilling, F., Borm, G., Würdemann, H., Möller, F., Kühn, M., CO_2SINK Group, 2009. Status report on the first European on-shore CO_2 storage site at Ketzin (Germany). Energy Procedia 1, 2029–2035.

Shukla, U.K., Bachmann, G.H., Singh, I.B., 2010. Facies architecture of the Stuttgart Formation (Schilfsandstein, Upper Triassic), central Germany, and its comparison with modern Ganga system, India. Palaeography, Palaeoclimatology, Palaeoecology 297, 110–128.

Wiese, B., Böhner, J., Enachescu, C., Würdemann, H., Zimmermann, G., 2010. Hydraulic characterisation of the Stuttgart Formation at the pilot test site for CO_2 storage, Ketzin, Germany. International Journal of Greenhouse Gas Control 4 (6), 960–971.

Wolfgramm, M., Rauppach, K., Seibt, P., 2008. Reservoirgeologische Charakterisierung mesozoischer Sandsteine im Norddeutschen Becken auf Basis petrophysikalischer und petrographischer Daten. Zeitschrift fur Geologische Wissenschaften 4 (5), 249–266.

Wu, Q., Xu, H., Zou, X., 2005. An effective method for 3D geological modeling with multi-source data integration. Computers & Geosciences 31, 35–43.

Würdemann, H., Möller, F., Kühn, M., Heidug, W., Christensen, N.P., Borm, G., Schilling, F.R., CO_2SINK Group, 2010. CO_2SINK – from site characterization and risk assessment to monitoring and verification: one year of operational experience with the field laboratory for CO_2 storage at Ketzin, Germany. International Journal of Greenhouse Gas Control 4, 938–951.

Wurster, P., 1964. Geologie des Schilfsandsteins, vol. 33. Mitt. Geol. Staatsinst., Hamburg, 140 p.

Yordkayhun, S., Ivanova, A., Giese, R., Juhlin, C., Cosma, C., 2009a. Comparison of surface seismic sources at the CO_2SINK site, Ketzin, Germany. Geophysical Prospecting 57, 125–139.

Yordkayhun, S., Juhlin, C., Norden, B., 2009b. 3D seismic reflection surveying at the CO_2SINK project site, Ketzin, Germany: a study for extracting shallow subsurface information. Near Surface Geophysics 7, 75–91.

Yordkayhun, S., Tryggvason, A., Norden, B., Juhlin, C., Bergman, B., 2009c. 3D seismic traveltime tomography imaging of the shallow subsurface at the CO_2SINK project site, Ketzin, Germany. Geophysics 74, G1–G15.